Journal of Medicinal Chemistry

Perspective

pubs.acs.org/jmc

Current Landscape of Phosphodiesterase 10A (PDE10A) Inhibition

Thomas A. Chappie,* Christopher J. Helal, and Xinjun Hou

Neuroscience Medicinal Chemistry, Pfizer, Inc., 700 Main Street, Cambridge, MA 02139, United States

The cyclic nucleotide phosphodiesterases (PDEs) are a multifamily class of enzymes that have garnered a significant amount of attention within the biotechnology and pharmaceutical industries over the past ~30 years. Modulation of these enzymes has provided the industry with successful drugs for the treatment of patients with heart failure (milrinone), chronic obstructive pulmonary disease (COPD) (roflumilast), erectile dysfunction (sildenafil, tadalafil, vardenafil), and pulmonary hypertension (sildenafil). Given the success of these programs, the inhibition of phosphodiesterases is a significant focus of many in the health care field.

cAMP (3′,5′-cyclic adenosine monophosphate) and cGMP (3′,5′-cyclic guanosine monophosphate) are second messengers within cells. These signaling molecules can be generated in two ways. They can carry signals generated by extracellular signaling molecules that are incapable of entering the cells. These extracellular signaling molecules, such as hormones or neurotransmitters, bind to membrane bound proteins that in turn activate the particulate forms of adenylate or guanylate cyclase. This activation results in the generation of cAMP or cGMP from adenosine triphosphate (ATP) and guanosine triphosphate (GTP), respectively (Figure 1). Soluble (cytosolic) forms of adenylate and guanylate cyclase also exist and can be activated by messengers within the cell. Soluble adenylate cyclase is activated by calcium signaling to generate cAMP, and soluble guanylate cyclase is activated by nitric oxide (NO) which in turn generates cGMP. The generation and resulting regulation of this signaling are important to many functions throughout the cell. Temporal and spatial regulation of cAMP and cGMP falls to the phosphodiesterases. This is done through the hydrolysis of cAMP and cGMP into their nonsignaling forms AMP and GMP, respectively.

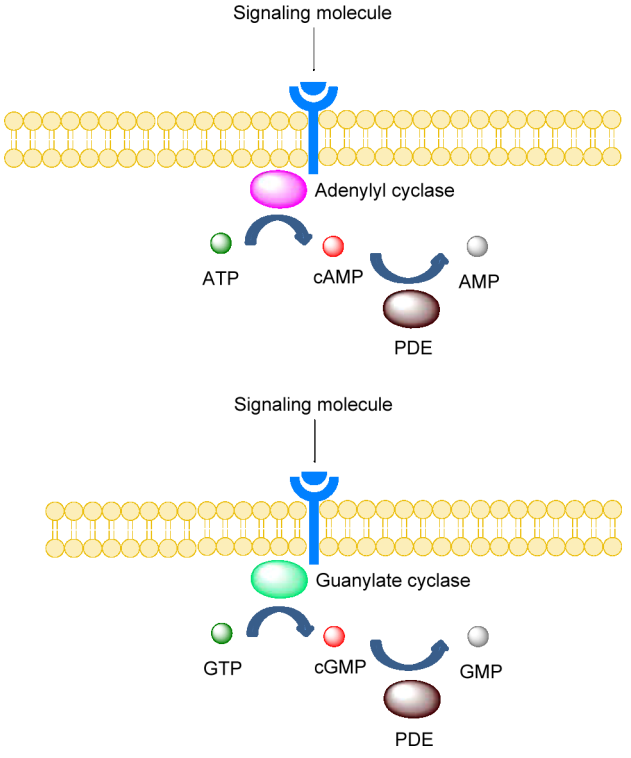

Figure 1. Generation of cyclic nucleotides through extracellular signaling and hydrolysis by a phosphodiesterase.

Phosphodiesterases consist of 11 families and are classified by the cyclic nucleotide substrate (cAMP and/or cGMP) that they hydrolyze (Figure 2). PDEs 1, 2, 3, 10, and 11 are dual substrate

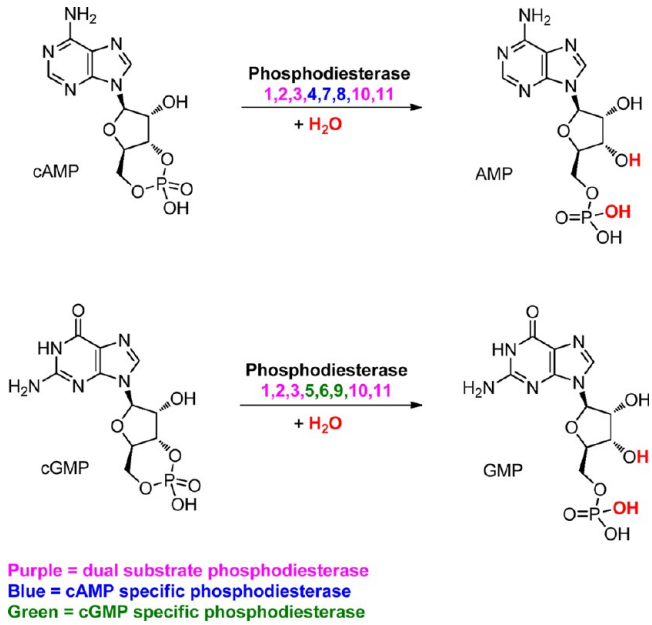

Figure 2. Hydrolysis of cAMP and cGMP to AMP and GMP.

enzymes, while PDEs 4, 7, and 8 hydrolyze only cAMP and PDEs 5, 6, and 9 hydrolyze only cGMP. Some families are further defined by subtype, such as PDE1A/B/C, PDE3A/B, PDE4A/B/C/D, PDE7A/B, and PDE8A/B, each encoded by a distinct gene. There are even further isoform classifications based on splice variants from individual genes that expand the phosphodiesterases to over 60 isoforms.

PDE10A is a single family member phosphodiesterase that is highly expressed in the striatum, a part of the basal ganglia system thought to play a role in regulating the response to external

Received: April 12, 2012
Published: July 26, 2012

dx.doi.org/10.1021/jm3004976 | J. Med. Chem. 2012, 55, 7299−7331

stimuli and some aspect of executive function. It was first discovered in 1999 by several groups.[1−4] Its high striatal expression made it a prime target for neuroscience disease indications where striatal disregulation was implicated. A recent disclosure using sophisticated quantification methodologies has verified that PDE10A expression in mouse striatum is highest among all the PDEs as measured by mRNA (Figure 3).[5] This high abundance of PDE10A mRNA in brain is also present in humans.[6]

The immunohistochemical localization of PDE10A in several mammalian species has been described.[7,8] These data are in good correlation with the mRNA data described in Figure 3.

PDE10A exists as two splice variants, PDE10A1 and PDE10A2.[9] The A2 splice variant is more prevalent than A1 in human brain. The significant differences in the N-terminus of the two proteins provides for different behaviors such as subcellular localization (Figure 4). PDE10A1 has been found primarily in the cytosol, and PDE10A2 is found primarily in membrane associated fractions of transfected PC12 cells.[10] A significant advance in our understanding of the cellular distribution of PDE10A2 was recently described by Charych et al.[11] They propose that at the local level of PDE10A2 protein production, high levels of cAMP result in phosphorylation at Thr-16 that keeps the PDE10A2 protein in the cytosol to lower local levels of cAMP concentrations. Under low local levels of cAMP, PDE10A2 is palmitoylated at Cys-11 and transferred to the axon or dendrite to regulate neurotransmitter signaling.

The PDE10A enzyme has two GAF domains. GAF A and GAF B domains combine to regulate the catalytic activity of PDEs through the allosteric, noncatalytic binding to cyclic nucleotides. The GAF B domain of PDE10A can bind cAMP. But a thorough in vitro characterization of the cAMP binding event to the GAF B domain of PDE10A found no activation of the enzyme.[12] An in vivo characterization will be needed to rule out phosphorylation states and binding partners that could account for the lack of in vitro activation. A review of the structural aspects of the phosphodiesterase associated GAF domains was recently published.[13] The catalytic site of the enzyme is well characterized and will be detailed in a later section.

Understanding the biological consequences of PDE10A inhibition is an active area of interest. A complete data package on the biochemical and behavioral activity of the selective PDE10A inhibitor **1** (TP-10, Figure 5) was first described in 2008.[14] **1** produces clear, dose responsive increases of cGMP, cAMP, and pCREB in mouse striatum. **1** has activity in preclinical antipsychotic models such as conditioned avoidance response (CAR), decreases in spontaneous locomotor activity (SLA), and phencyclidine (PCP)- and amphetamine (AMPH)-stimulated locomotor activity. This is a very similar set of activities to clinically efficacious antipsychotic agents (Table 1). One behavioral model that is not affected by **1**, but that is affected by D_2 antagonists, was paired pulse inhibition (PPI) and reversal of **2** (MK-801, Figure 6)[15,16] induced PPI.[14,17] The lack of activity in PPI as first described in 2008 is contrary to other reports of PDE10A activity in these models and models where PDE10A inhibition reverses **2** induced deficits. Reduced catalepsy was observed as compared to D_2 antagonists, which suggests the potential for minimized extrapyramidal side effects versus marketed antipsychotic drugs.

PDE10A inhibitors have been behaviorally characterized in many preclinical rodent models. A compilation of all the behavioral models used to characterize PDE10A inhibitors described in patents and publications is highlighted in Table 2.

The data in the report were accompanied by a hypothesis to account for the activity that is seen from PDE10A inhibition. PDE10A inhibitors, like D_2 antagonists, activate brain circuits involved in dampening behavioral reactivity (D_2 indirect or striatopallidal pathway). But unlike D_2 antagonists, PDE10A inhibitors also increase the activity of neurons involved in the initiation of behavioral responses to salient stimuli, the D_1 direct pathway. These two pathways are generally considered to be antagonistic, but their dual activation through PDE10A inhibition is thought to provide unique therapeutic potential. A more detailed account of this hypothesis can be found in a previous 2009 review.[19]

A mouse brain glucose metabolism study with **5** (MP-10)[20] provides more data to support this hypothesis.[21] A D_1 agonist (direct pathway), **4** (SKF 82958),[22,23] shows a dose dependent increase in activation of the globus paladus, while a D_2 antagonist (indirect pathway), haloperidol, shows a dose dependent increase in activation of the lateral habenula. The PDE10A inhibitors **5**, papaverine,[24] and **6** (PQ-10)[25] (Figure 7) cause increased activation in both the globus paladus and the lateral habenula, consistent with activation of both direct and indirect pathways. One important note from this paper is that the activation of the lateral habenula (D_2 pathway) with **5** was optimal at a dose of 0.63 mg/kg and was diminished with increasing doses to give a bell shaped curve. This bell shaped curve phenomenon was not seen with haloperidol, where a dose-dependent increase in activation was seen. The same 0.63 mg/kg dose of **5** also provided a dose-dependent, statistically significant activation of the globus paladus (D_1 pathway). This suggests that differing exposures of **5** could elicit different responses based on the amount of activation in each pathway. If these activation pathways translate to higher species, monitoring glucose metabolism may be an important tool for setting doses in the clinic.

Beyond the strong rational for antipsychotic activity of PDE10A inhibitors, there is an emerging set of preclinical data indicating the potential for treatment of patients with Huntington's disease. Kleiman et al. have recently described the consequences of long-term PDE10A inhibition on gene expression in the mouse striatum.[26] They describe altered gene expression in 19 genes, activity in a striatum-located CRE-luciferase reporter that highlights CREB mediated striatal activation, and increases to the phosphorylation of several proteins such as mitogen- and stress-activated kinase 1 and histone 3 (H_3). Taken as a whole, the authors suggest that PDE10A inhibition may also have neuroprotective activity. A second report describes the activity of PDE10A inhibitor **1** in the mouse R6/2 model of Huntington's disease.[27] Following dosing of **1** from week 4 until study end, the researchers saw significant neuroprotection in all measured parameters thought to be relevant to reversal of the disease.

Given the high CNS expression of PDE10A, there has been limited research into the peripheral aspects of PDE10A inhibition. One new report describes PDE10A inhibition as a potential treatment for pulmonary hypertension.[28] Chronic dosing of the PDE10A inhibitor papaverine in rats resulted in 40−50% attenuation of monocrotaline induced pulmonary hypertensive hemodynamic parameters and pulmonary vascular remodeling. In vitro studies with papaverine and PDE10A siRNA suggest that this affect is cAMP mediated.

In 2005 there were a series of patent applications that described the use of PDE10A inhibitors for the treatment

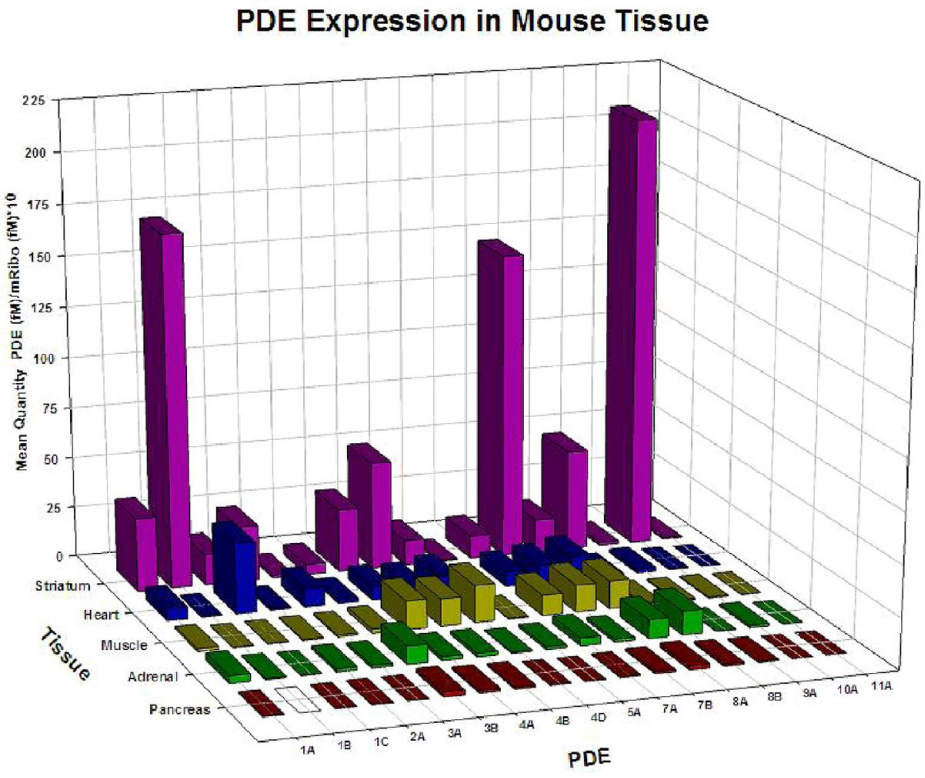

Figure 3. mRNA PDE expression in mouse tissue.

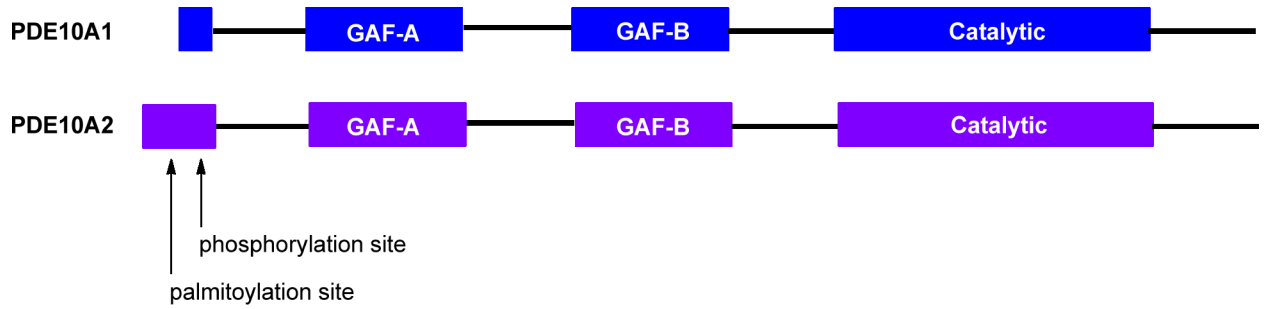

Figure 4. Representation of PDE10A enzyme structure.

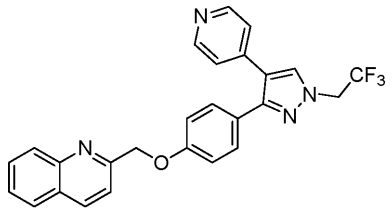

Figure 5. PDE10A tool compound **1**.

metabolic related diseases such as diabetes and obesity. Two of the applications describe the effects of PDE10A inhibition on glucose levels,[29,30] while one describes the resistance of PDE10A treated rats to weight gain while on a high fat diet.[31] Most companies patenting PDE10A inhibitors since that time claim treatment of metabolic diseases as an indication and use these reports to support the claims. And there have been no additional follow-up literature reports of the effects of PDE10A inhibition on metabolic diseases.

Table 1. Activity Comparison of Marketed Antipsychotics and PDE10A Inhibitor 1 in Rodent Models of Psychosis with Acute Dosing[a]

	rat					mouse
	CAR	SLA	PCP LA	AMPH LA	PPI	**2** induced PPI reversal
haloperidol	0.04	0.07	0.13	0.02	0.32	
ziprasidone	0.52	0.71	0.20	0.17	1.78	
risperidone	0.13	1.06	0.15	0.07	1.0	1.0
clozapine	5.0	1.63	1.80	0.87	0.56	
1	1.1	1.4	0.69	2.6	no effect	no effect

[a]Shown are CAR (conditioned avoidance response), SLA (spontaneous locomotor activity), PCP LA (phencyclidine locomotor activity), AMPH LA (amphetamine locomotor activity), PPI (prepulse inhibition), and **2** induced PPI deficit. All activities are ED_{50} values (mg/kg sc).

dx.doi.org/10.1021/jm3004976 | J. Med. Chem. 2012, 55, 7299−7331

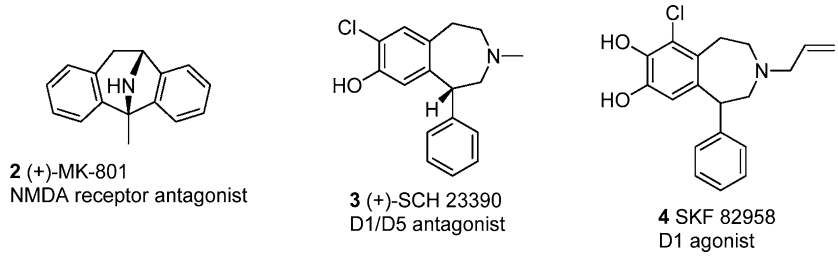

Figure 6. Pharmacological agents used to understand the PDE10 inhibition pathway.

Table 2. Rodent Behavioral Assays Used for Characterization of PDE10A Inhibitors

behavioral model (rat)	behavioral model (mouse)
conditioned avoidance response (CAR)	conditioned avoidance response (CAR)
spontaneous locomotor assay (SLA)	prepulse inhibition (PPI)
apomorphine induced stereotypy	**2** induced PPI
apomorphine induced PPI	**2** induced hyperactivity
PCP induced locomotor assay	**3** (SCH 23390)[18] hypolocomotion
novel object recognition	novel object recognition
2 induced hyperactivity	forced swim
2 induced stereotyped sniffing	light and dark box
amphetamine locomotor assay	

■ ENZYME STRUCTURE

Medicinal chemistry efforts to develop PDE10A inhibitors have been a model example of the use of structure based drug design (SBDD) techniques in the generation of potent and selective inhibitors. Since the beginning of the design of PDE10A inhibitors, a crystal structure of the catalytic subunit of PDE10A has been available to the medicinal chemistry community.[32] We rationalized a medicinal chemical strategy to leverage this rich structural information to deliver multiple lead series with diverse binding modes. It was felt that a deep understanding of the inhibitor−PDE10A enzyme interaction could provide useful information with regard to specific binding modes and the activity and selectivity that resulted. Several of these studies have now been published.[20,25,33] A specific but as yet unrealized area of interest is in understanding the different types of binding modes and the biological impact, if any, these different binding modes can impart to the biological consequences of PDE10A inhibition. One can imagine that certain classes of inhibitors could change the overall structure of the enzyme−inhibitor complex and thus influence the binding partners, localization, and eventual biological effect of PDE10A inhibition. While this is purely speculation for PDE10A inhibition, the phenomenon of differing inhibitor binding modes on the biological activity of PDEs has been documented in PDE4A.[34]

To map out the structure of the catalytic subunit of PDE10A, we can begin by looking at a crystal structure of the product of PDE10A hydrolysis, AMP, bound to the human enzyme (Figure 8).[35] There are three major areas of recognition: (i) phosphodiesterase invariant glutamine−adenosine dual H-bond interaction, (ii) occupation of the hydrophobic clamp by the fused biaryladenosine system, and (iii) interactions between the ribofuranose phosphonate group with catalytic metal/water complex. Inherent in all phosphodiesterases is a glutamine (Gln) residue that is responsible for hydrogen-bonding to the enzyme substrate, whether cAMP or cGMP. In the crystal structure (Figure 8), recognition of AMP requires the carbonyl of the Gln amide side chain to accept a hydrogen bond from the adenine 6-NH_2 group while the amine of the Gln amide side chain

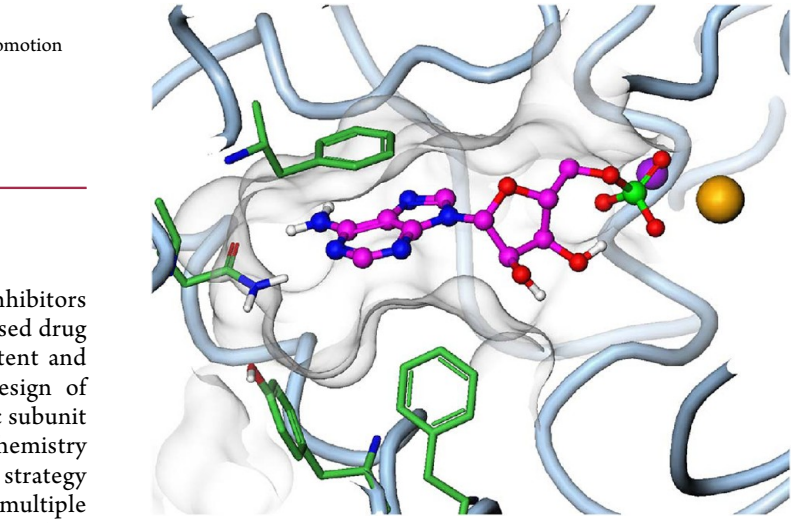

Figure 8. AMP cocrystallized in the PDE10A catalytic site (PDB entry 2OUN).

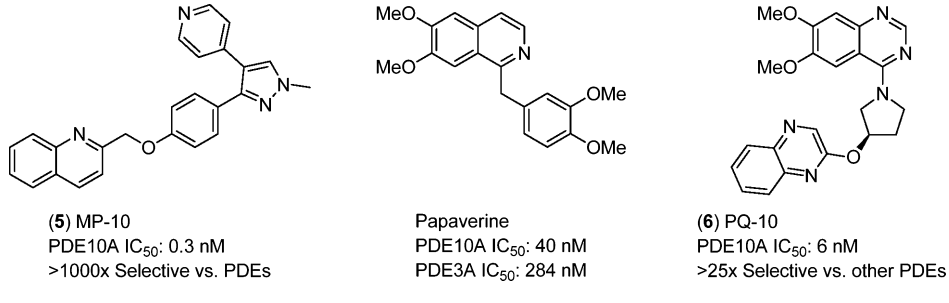

Figure 7. PDE10A inhibitor reference compounds.

dx.doi.org/10.1021/jm3004976 | J. Med. Chem. 2012, 55, 7299−7331

donates a hydrogen bond to N-1 of the adenine ring. Recognition of cGMP would require the invariant Gln side chain to donate a hydrogen bond from the amino group to the C-6 carbonyl of the guanine while the Gln amide carbonyl would accept a hydrogen bond from the $-N_1H$ of the guanine ring. The orientation of the Gln in Figure 8 is consistent with the recognition of cAMP. For PDE10A to recognize cGMP, the orientation of the Gln amide side chain would have to be reversed. There has been debate in the field as to whether the Gln is free to rotate to accommodate both cyclic nucleotide substrates in dual substrate PDEs, is locked in one of the two conformations in cAMP or cGMP specific PDEs, or is locked in only one conformation, and the differences of the catalytic subunit of the enzymes allow for the substrate to bind in a different orientation.[19]

Reports of inhibitor X-ray cocrystal structures have been published and provide a significant three-dimensional data set that has helped to provide multiple options for the prospective design of selective PDE10A inhibitors. Two quite different inhibitor binding modes, as exemplified by **5**[20] and **6**[25] (Figure 9), can be used to describe general elements of binding that are important for PDE10 inhibition. **6** and other dimethoxycatechol type inhibitors such as papaverine make a bidentate hydrogen bond with the conserved Gln via the dimethoxy group, while the quinazoline ring occupies the hydrophobic clamp (Figure 9). A third element of the binding of **6** is the pendent fused biaryl group which makes subtle hydrophobic interactions with PDE10A outside the enzyme catalytic site, which can be described as exo-binding. The X-ray structure of **5** provided particularly important structural information with the discovery of the PDE10A "selectivity pocket" (Figure 9).[20] Among the PDEs, three features define the unique characteristics of this pocket and allow for generating inhibitors with high PDE10A specificity. First, among all 21 members of the PDE family, only PDE10A has a Gly-715 (rat residue numbering), next to the conserved glutamine (Gln-716). The presence of a larger side chain in all other PDEs blocks access to the pocket. Second, the residues that form the back of this lipophilic pocket are from the M-loop, which connects helix 14 and helix 15.[32] An insertion at this loop of PDE10A (Lys/Arg-709) results in a deeper pocket in PDE10A. Finally, PDE10A has Tyr-683 to form a hydrogen bond interaction with which to anchor an inhibitor in the selectivity pocket. While some PDEs may have some features, such as longer M-loop in PDE5/6 or tyrosine in PDE2, only PDE10A has all three combined features, creating the unique PDE10A selectivity pocket. This pocket has been shown to accommodate substituted aryl ring systems. A hydrogen bond acceptor as part of the aryl group must be present to anchor the inhibitor. Aryl groups lacking the appropriate H-bond acceptor have little to no measurable enzyme inhibition. The pyrazole ring of **5** does occupy a portion of the hydrophobic clamp. Lastly, a pyridyl ring makes a key H-bond to a water molecule that is an integral part of the structure of the enzyme. This H-bond can account for a significant amount of potency from this inhibitor class. Interestingly, **5** is one of the few PDE10A inhibitors that does not form a traditional hydrogen bond with the invariant Gln.

By combinination of the structural information gained from the enzyme inhibitor X-ray cocrystals of the endogenous enzymatic product, AMP, and several known inhibitor classes, a two-dimensional (2D) representation of the known elements of PDE10A inhibition can be generated. In Figure 10 the blue line approximates the boundary of the cavity that exists in the

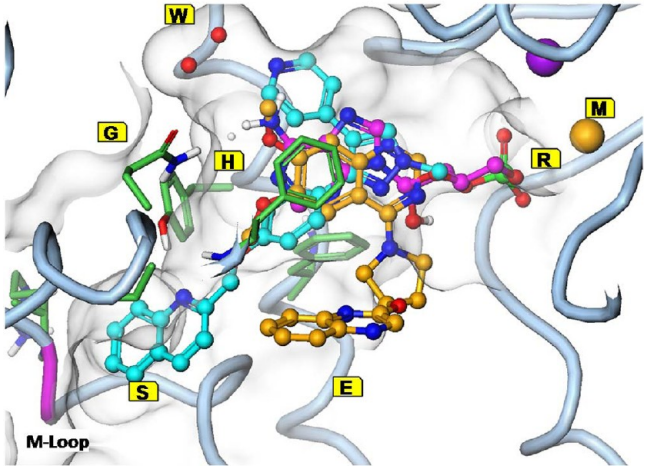

Figure 9. Overlay of AMP (magenta), **5** (cyan), and **6** (orange) in the catalytic site of PDE10A, with identification of the interactions or regions thought to be important for PDE10A inhibition: W = buried waters, M = metals, R = ribose site, H = hydrophobic clamp, G = invariant glutamine, S = selectivity pocket, E = exo-binding site. PDB entries are 2OUN, 2OVY, and 3HR1.

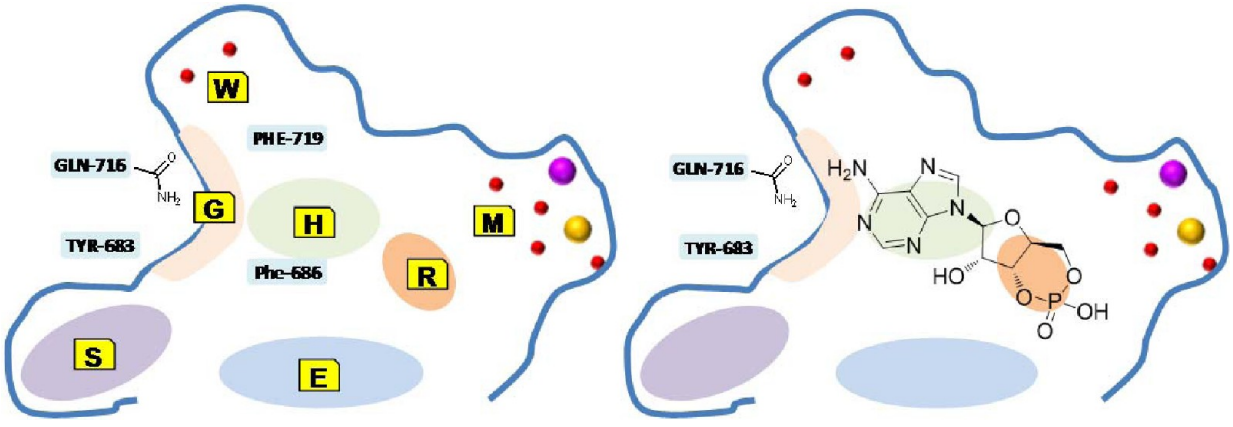

Figure 10. (Left) A two-dimensional (2D) representation of elements or regions shown to be important for PDE10A inhibition. (Right) A 2D representation of the endogenous substrate cAMP bound to PDE10A. Labels are defined as follows: G (Gln interaction), S (selectivity pocket), H (hydrophobic clamp), W (buried waters), M (metal site), R (ribose region), E (exo-binding region).

dx.doi.org/10.1021/jm3004976 | J. Med. Chem. 2012, 55, 7299–7331

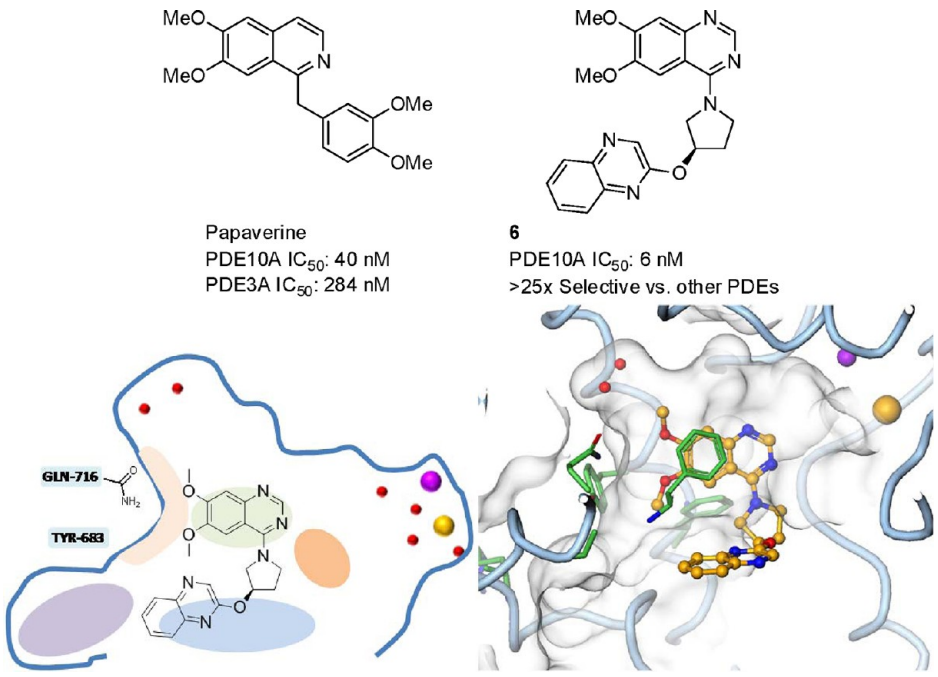

Figure 11. A 2D and 3D representation of **6** in the PDE10A catalytic site (PDB entry 2OVY).

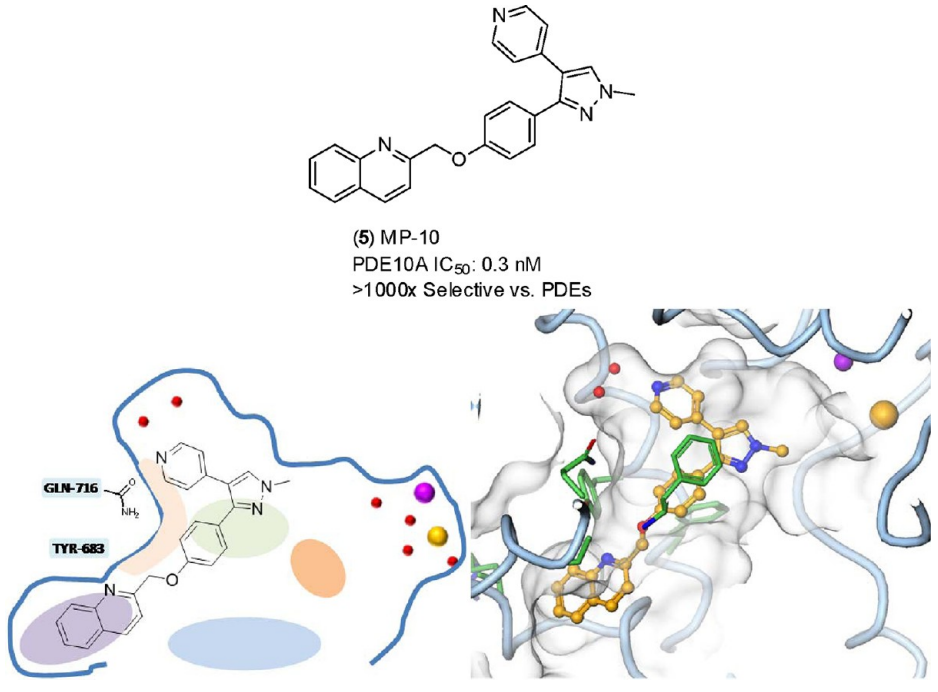

Figure 12. A 2D and 3D representation of **5** in the PDE10A catalytic site (PDB entry 3HR1).

catalytic subunit of PDE10A. G represents the invariant Gln that is critical for cAMP/cGMP recognition. H represents the hydrophobic clamp area that recognizes the adenosine or guanosine ring systems of cAMP and cGMP, respectively. M represents the area in the enzyme that contains the metals used to catalyze the hydrolysis of cAMP and cGMP. These metals contain a highly ordered water network that could be utilized for designing inhibitor H-bond interactions. Additionally, R represents the ribose region. This area could be used as a potential point of incorporation of high stereocomplexity and to differentiate an inhibitor from the two-dimensional planar structures that are the bulk of the disclosed PDE10A inhibitors. E signifies the exo-binding site highlighted by **6** (Figure 11) in which hydrophobic interactions with the protein outside the catalytic site can be used for potency gain as well as modest selectivity gains. S indicates the selectivity pocket of PDE10A first described by **5** and the nearby Tyr-683 (rat) that anchors the successful occupation of the selectivity pocket through the donation of a hydrogen bond. Finally, W represents the water molecules that are integral to the structure of the PDE10A enzyme and pose a significant opportunity for potency enhancement through successful H-bond interaction.[36] Not all elements need to be satisfied for inhibition of the enzyme. This graphic is intended only to show the areas of the enzyme that have been or

dx.doi.org/10.1021/jm3004976 | J. Med. Chem. 2012, 55, 7299−7331

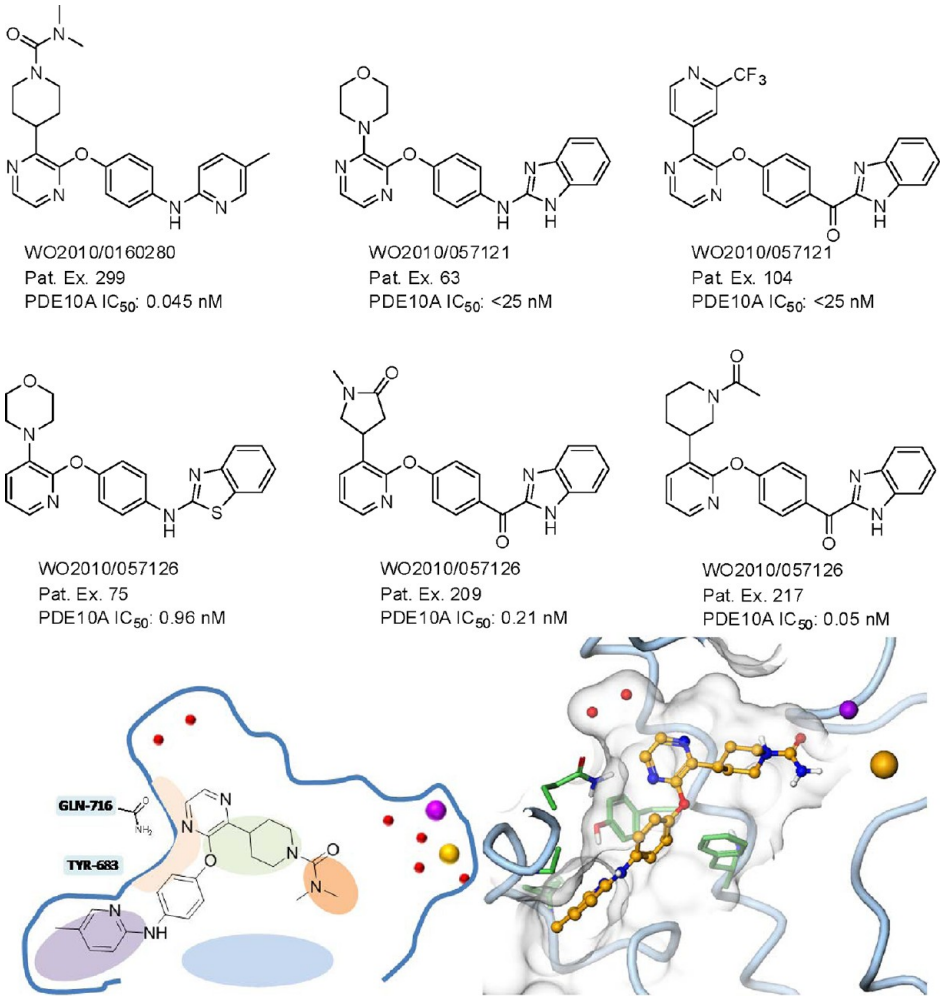

Figure 13. Representative compounds disclosed in three patent applications by Amgen in 2010 and a 2D and 3D representation of the proposed binding elements.

could be exploited in the design of potent and selectivity inhibitors. The advantage of the two-dimensional representation shown in Figure 10 is that it can be used to describe interactions with PDE10A inhibitors and the enzyme in a shorthand, easy-to-interpret manner.

■ PDE10A INHIBITORS

We have endeavored to provide an overview of the literature and patent reports of PDE10A inhibitors with a focus on 2009–2011. Examples that have been chosen and highlighted from each report are not meant to be comprehensive and should not be interpreted as the author's estimation of the best compound or compounds from that particular patent, patent application, or literature report. The examples have been chosen as a reference point to highlight the chemical matter within the report as an interesting SAR trend or simply because the authors of the original report have highlighted them and provided additional data. The three-dimensional modeling and docking results are based on X-ray cocrystal structures of the rat PDE10A enzyme. For the purposes of this review, we have not reported details of the enzymatic assays. Details such as the species in which the PDE10A enzyme is derived, enzyme concentrations, and temperatures are contained within the Supporting Information or details of the invention sections of the appropriate reference.

The first disclosed inhibitor of PDE10A was the natural product papaverine.[37,38] Early directed designs of inhibitors had structural elements similar to those of papaverine, such as a dimethoxycatechol bidentate interaction with the conserved Gln, the occupation of the hydrophobic clamp, and a pendent aryl group that could interact with residues outside the catalytic site (Figure 11). The first of these to be published was **6**, a potent and moderately selective in vivo active PDE10A inhibitor.[25]

The second generation of PDE10A inhibitors was highlighted by the discovery of **5** (Figure 12).[20] This compound was important for several reasons. First, it was the first public disclosure of a PDE10A inhibitor in human clinical trials. Second, it informed the medicinal chemistry community of the existence of a "selectivity pocket" in proximity to the catalytic site of the PDE10A enzyme. Occupation of this pocket by the ligand provides nearly complete selectivity vs other PDEs. The PDE10A medicinal chemistry community has embraced the design of selectivity pocket inhibitors.

Most disclosed binding modes of PDE10A inhibitors have followed with several of the recognition elements described either by the endogenous substrate cAMP/cGMP and the similar papaverine-like inhibitors or by the more recently described "selectivity pocket" inhibitors. In highlighting inhibitors from institutions working in the area of PDE10A

dx.doi.org/10.1021/jm3004976 | J. Med. Chem. 2012, 55, 7299–7331

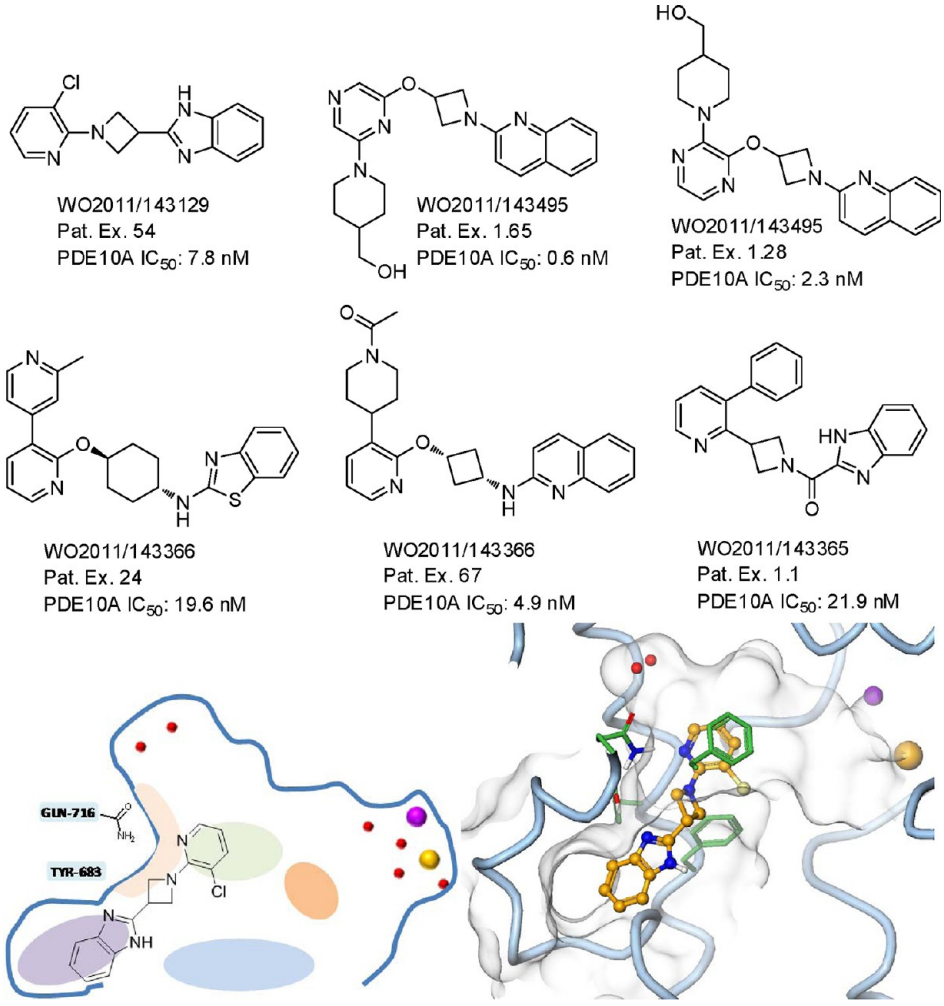

Figure 14. Representative compounds disclosed in three patent applications by Amgen in 2011 and a 2D and 3D representation of the proposed binding elements.

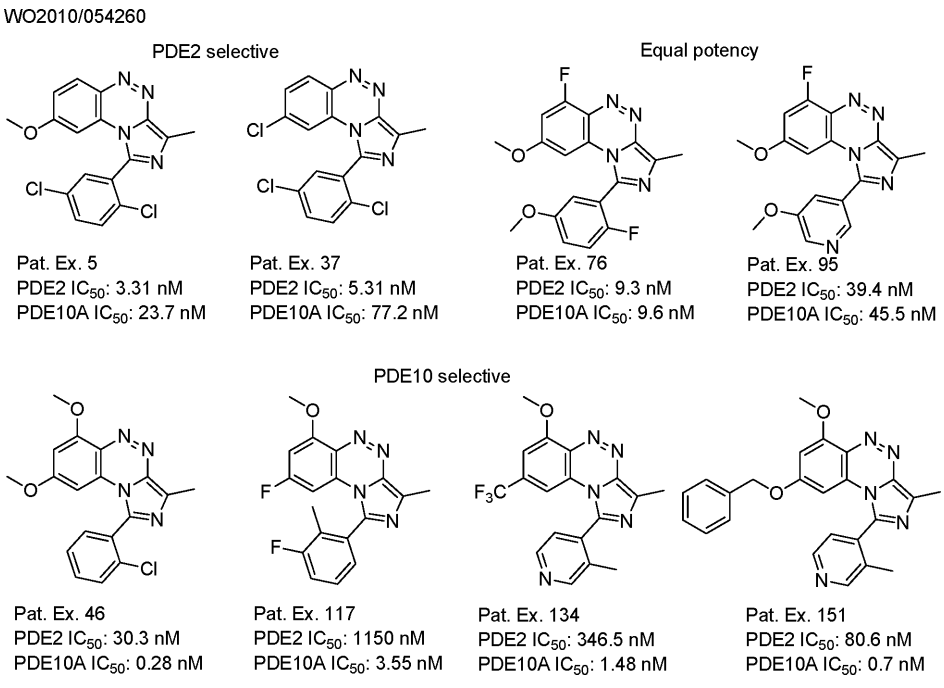

Figure 15. Examples of PDE10A inhibitors from Biotie/Wyeth.

dx.doi.org/10.1021/jm3004976 | J. Med. Chem. 2012, 55, 7299−7331

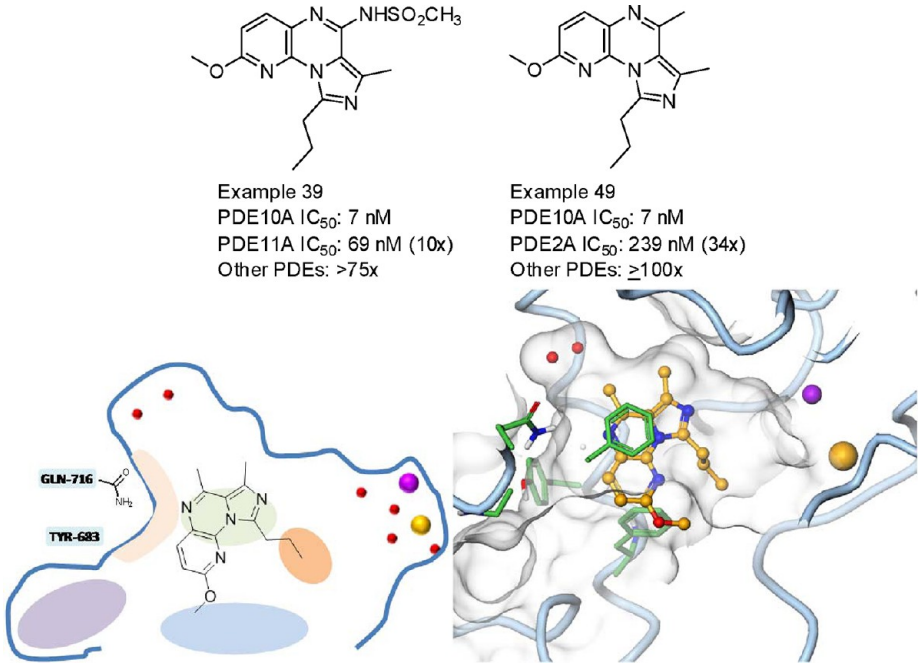

Figure 16. Example 39 and example 49 from a recent Biotie/Wyeth paper and the 2D and 3D representations of the binding mode (PDB entry 2LXG).

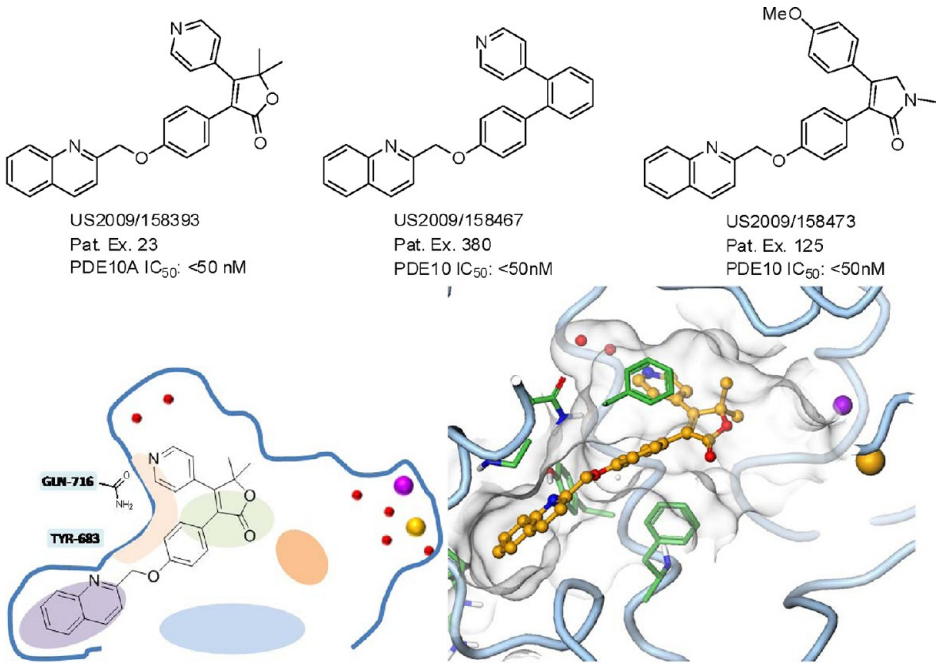

Figure 17. Examples of **5** inspired PDE10A inhibitors and a 2D and 3D representation of the proposed binding mode.

inhibitors, our focus will be on the strategies that are being implemented in designing new inhibitors. Structural information disclosed in publications, software modeling exercises, or knowledge of the enzyme structure will be used in trying to understand the types of inhibitor designs. Our focus will cover only disclosures from 2009 through mid-2011, as several reviews have captured efforts in the area prior to 2009.[19,39]

Amgen. There have been three patents filed from Amgen during 2010[40−42] and four filed in 2011.[43−46] Although binding modes of their inhibitors have not been disclosed, modeling suggests that these new series of PDE10A inhibitors are occupying the selectivity pocket of the enzyme. Representative compounds from each patent are shown in Figure 13. Common features are the central heteroaryl ring which could make an interaction with the invariant Gln and occupy some of the hydrophobic clamp. The high variability of the substituent at the 3-position of the central pyrazine or pyridine suggests this portion of the molecules is not making specific interactions with the enzyme and could therefore occupy a portion of the enzyme near the metals (Figure 13; Pat. Ex. 299, 63, and 104). In the patent applications disclosed in 2010, there is also a phenyl ring with a short spacer to a heteroaryl ring containing a hydrogen bond acceptor that presumably interacts with the Tyr, much like the selectivity pocket motif of **5**.

dx.doi.org/10.1021/jm3004976 | J. Med. Chem. 2012, 55, 7299−7331

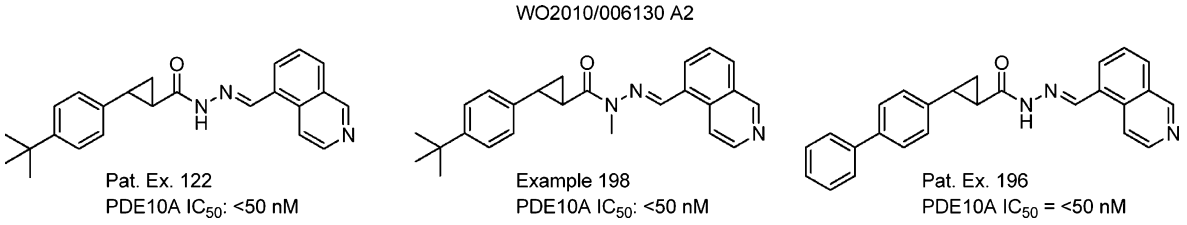

Figure 18. Representative hydrazide PDE10A inhibitors from EnVivo.

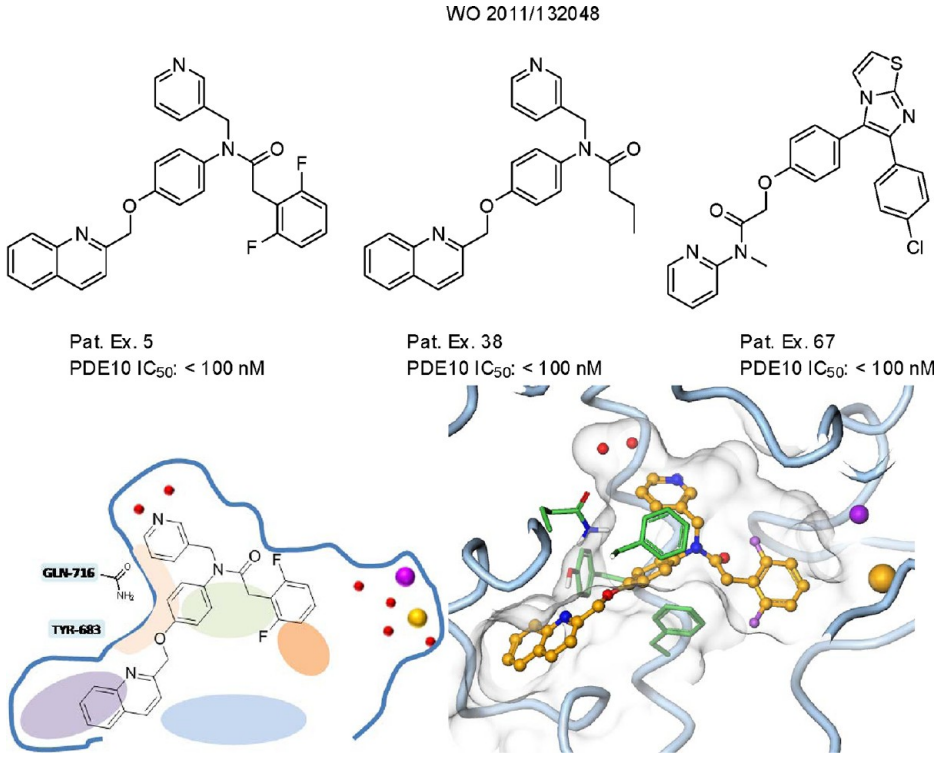

Figure 19. Examples of PDE10A inhibitors from Glenmark and a 2D and 3D representation of proposed binding modes.

In the Amgen patent disclosures from 2011, the bulk of the work is in the identification of the spacer region whose job is to correctly position the heteroaryl group that interacts with the Tyr of the selectivity pocket and the heteroaryl group that occupies the hydrophobic clamp and interacts with the invariant Gln through an H-bond acceptor motif (Figure 14).

This is an impressive array of compounds given the potency that is being reported. Additionally, there are also data indicating in vivo activity of these compounds in three rodent models of psychosis: CAR, apomorphine induced deficits of PPI, and reversal of PCP induced locomotor activity.

Excitingly, Amgen's Web site describes a PDE10A inhibitor in phase I studies. On the basis of the strong efforts highlighted above, they will certainly be taking forward a potent and selective PDE10A inhibitor.

Biotie/Wyeth. Biotie and Wyeth had partnered to generate some versatile PDE10A inhibitors (Figure 15). They have advanced a series of PDE10A inhibitors that do not interact with the selectivity pocket and therefore do not have exquisite selectivity, but in doing so, they have flexibility to tune the molecules to a desired activity. This is highlighted in a patent disclosed in 2010.[47] This patent describes a series of imidazotriazines with selectivity for PDE2A over PDE10A. There are several examples of compounds with equal potency for PDE2A and PDE10A. On the basis of the interest in PDE2 inhibitors as potential treatment for cognitive deficits associated with affec\tive disorders, it would be interesting to see the biological consequences of a dual PDE2A and PDE10A inhibitor.[48] Finally, they are able to tune several of these imidazotriazine inhibitors to PDE10A selectivity of >300×. Behavioral activity of this series of compounds is also described. Given the mixed pharmacology, it would be hard to ascribe the behavioral activity to any particular PDE activity or combination of activities.

The binding mode of a very similar series of imidazopyrazine PDE10A inhibitors was disclosed in a recent paper.[17] Two compounds from this series of inhibitors are highlighted, examples 39 and 49 (Figure 16). Both compounds share equivalent potency for PDE10A but differ in their selectivity profiles against other PDEs. Both compounds were active in the reversal of **2** induced hyperactivity and **2** induced stereotyped sniffing.

EnVivo. EnVivo published three patents in 2009 in which they devised variations on the pyrazole ring of **5** (Figure 12). These patents do not assign the exact potency versus PDE10A but instead provide a potency cutoff of IC_{50} greater than or less than 50 nM. Given the similarity to **5**, it is likely that these compounds are utilizing the selectivity pocket and are quite selective. Example 23[49] (Figure 17) has replaced the

dx.doi.org/10.1021/jm3004976 | J. Med. Chem. 2012, 55, 7299−7331

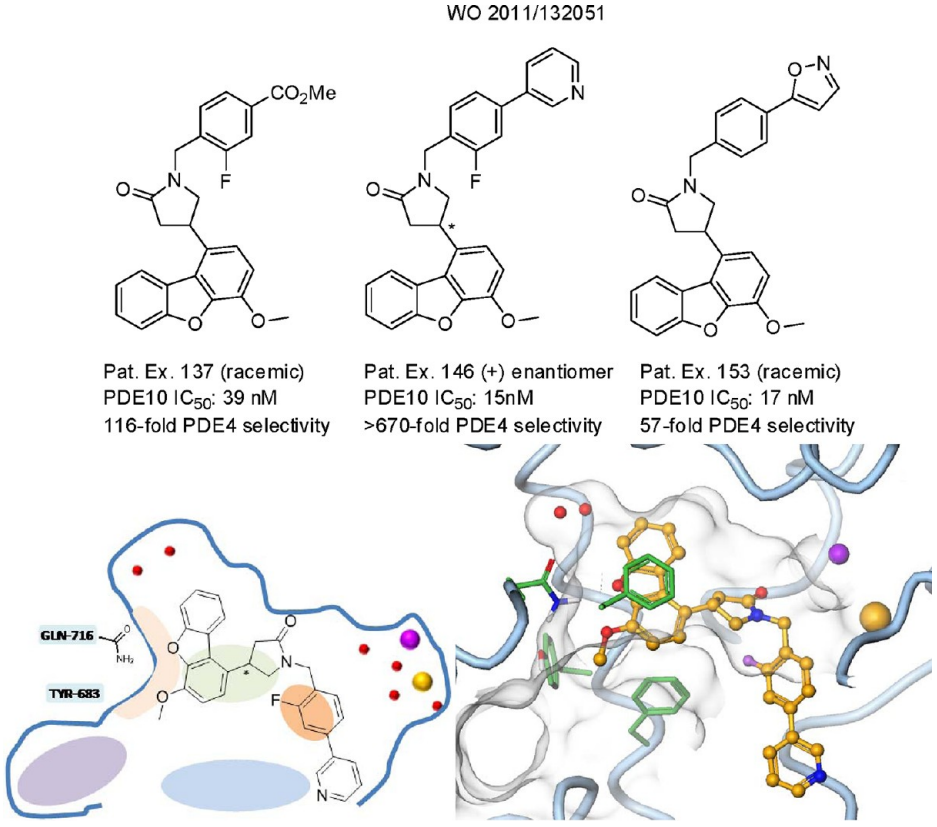

Figure 20. Examples of PDE10A inhibitors from Glenmark and a 2D and 3D representation of the proposed binding mode.

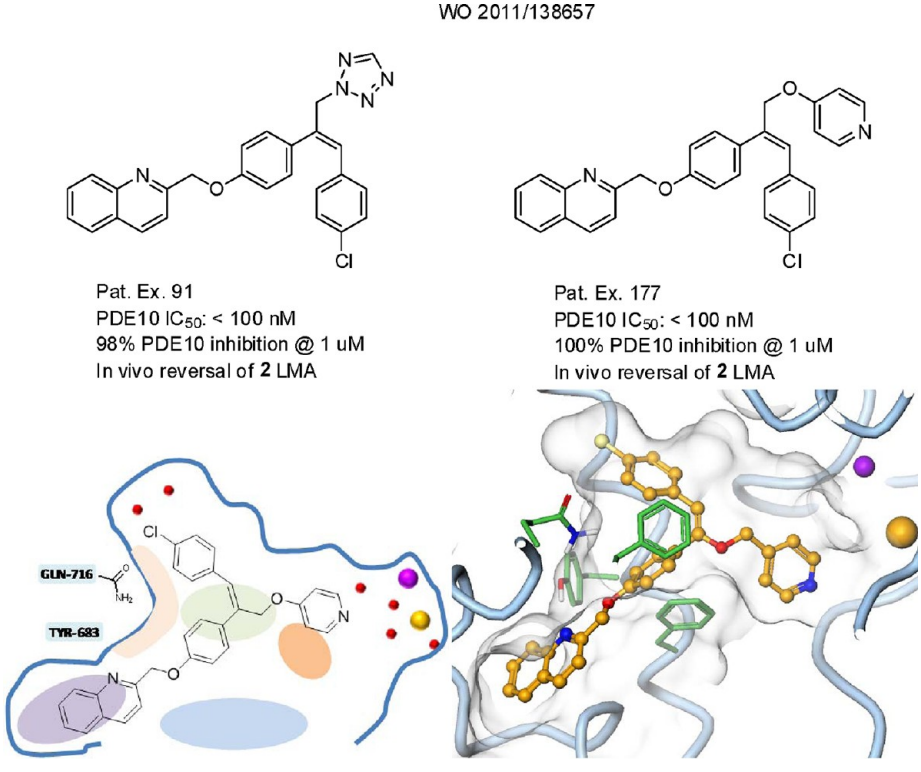

Figure 21. Examples of PDE10A inhibitors from Glenmark and the 2D and 3D representations of the proposed binding mode.

methylpyrazole ring with a furanone structure. Example 380[50] (Figure 17) replaces the pyrazole ring with a phenyl ring, with many substituents tolerated. An interesting finding is shown in example 125 where the pyridyl ring has been replaced with a methoxy substituent.[51] Given the strong interaction that **5**, and presumably EnVivo's PDE10A inhibitors, gains through the hydrogen bond to the water in the back of the enzyme (W), it would be interesting to see the binding potency number and

dx.doi.org/10.1021/jm3004976 | J. Med. Chem. 2012, 55, 7299−7331

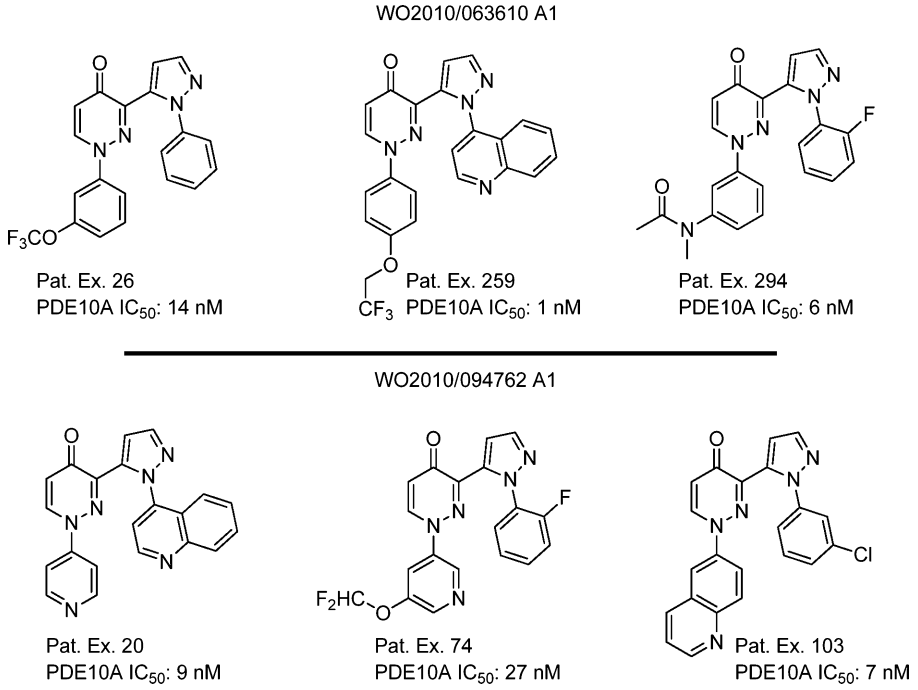

Figure 22. Representative structures from two Hoffmann-La Roche PDE10A inhibitor patents.

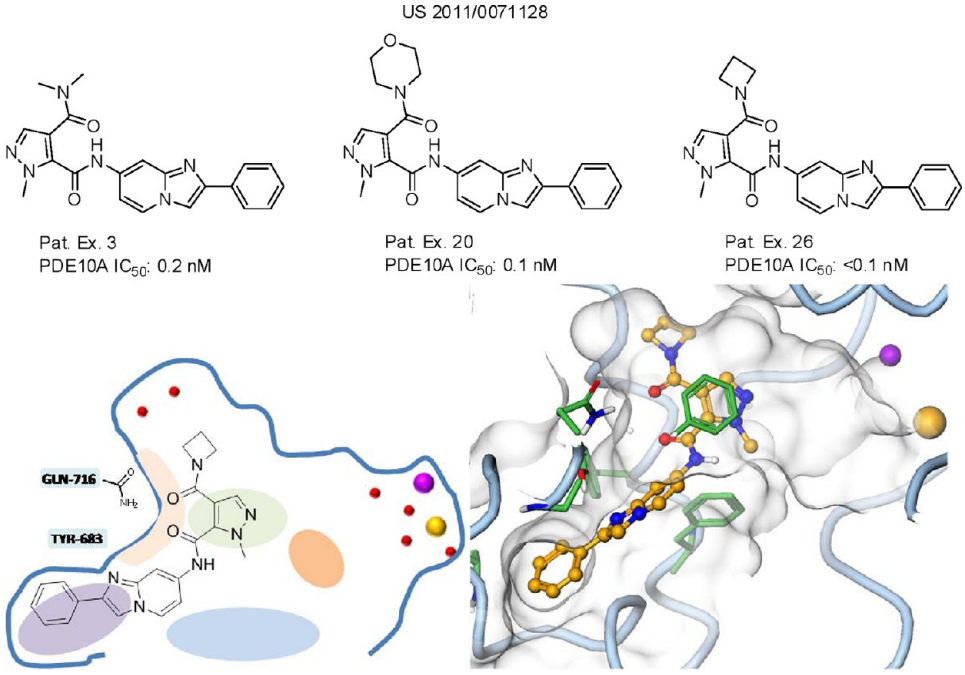

Figure 23. Examples of Hoffman-La Roche PDE10A inhibitors and a 2D and 3D model of the proposed binding mode.

X-ray crystallographic data to ascertain whether example 125 is making a H-bond to the water or whether it is replacing the water within the pocket. EnVivo describes these inhibitors as having a broad range of in vivo activity such as mouse CAR, mouse PPI, reversal of mouse **2** induced hyperactivity, and mouse catalepsy.

A structurally diverse PDE10A inhibitor was disclosed in a 2010 EnVivo patent (US2010/006130 A2).[52] There is a core cyclopropyl ring adjacent to a hydrazide. The SAR shows a portion of the inhibitors with a very lipophilic group off one carbon of the cyclopropyl (examples 122 and 198, *p*-^{t}Bu-phenyl; example 196, *p*-diphenyl; Figure 18). A hydrazide group is off another cyclopropyl carbon. A methyl substitution on the central nitrogen is apparently not detrimental to the geometry needed for inhibition, and it is able to keep its potency to <50 nM (example 198, Figure 18). No in vivo activity was provided with this patent. Because of the significantly different structures of these inhibitors compared to other PDE10A inhibitors, all attempts to discern a single favored binding mode were not successful.

dx.doi.org/10.1021/jm3004976 | J. Med. Chem. 2012, 55, 7299−7331

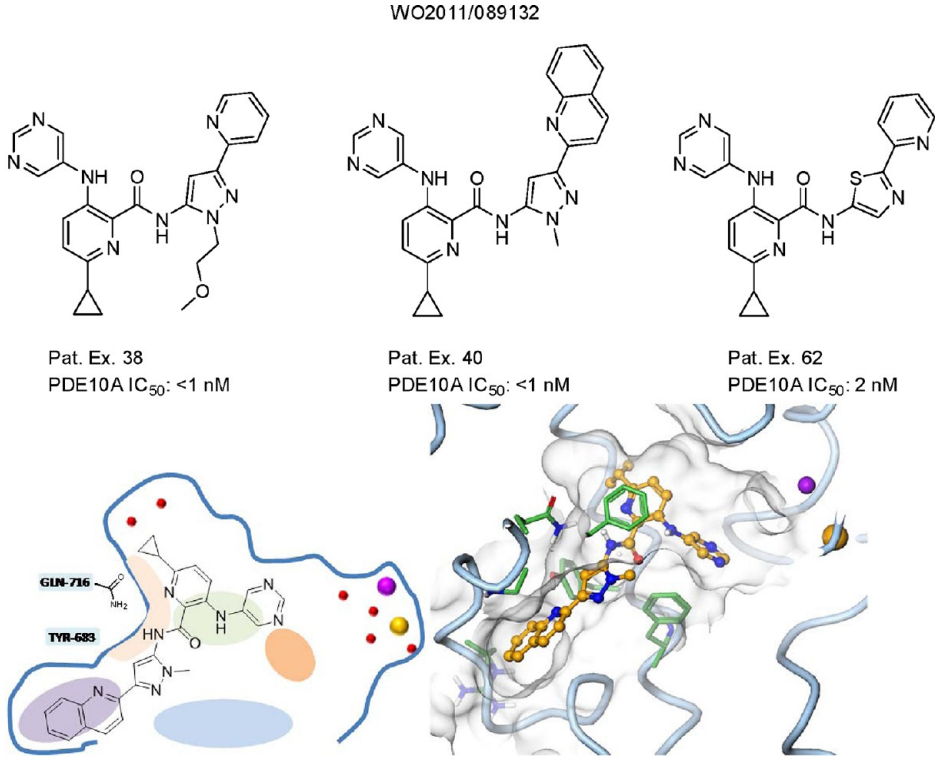

Figure 24. Examples of Hoffman-La Roche PDE10A inhibitors and a 2D and 3D model of the proposed binding mode.

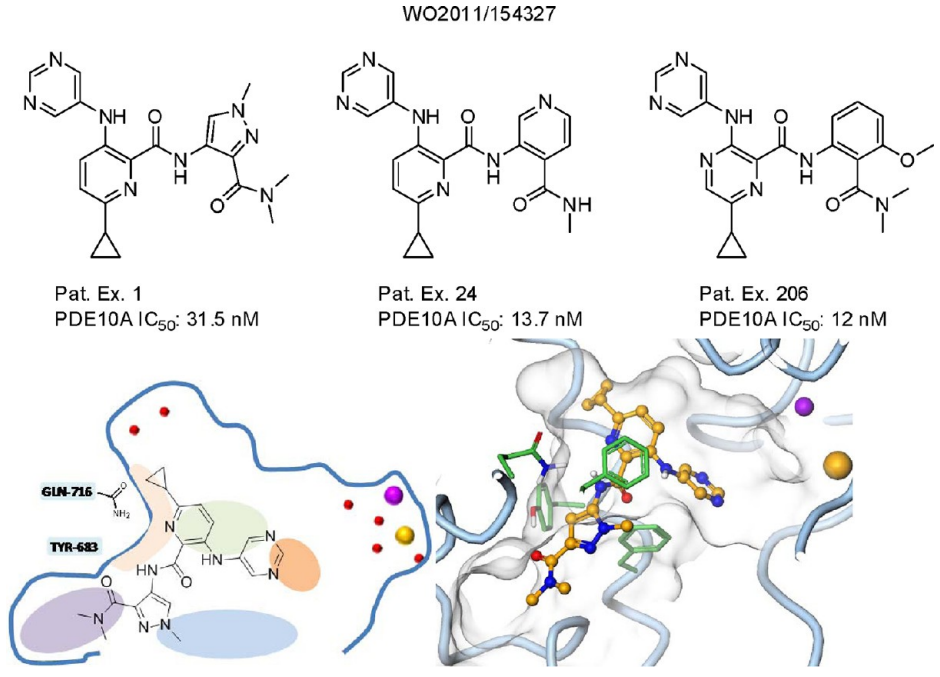

Figure 25. Examples of Hoffman-La Roche PDE10A inhibitors and a 2D and 3D representation of their proposed binding mode.

Glenmark. WO2011/132048 reveals 2-quinolylmethyloxy-arylamines that most likely bind in a similar manner to **5** with the quinolyl group occupying the selectivity pocket (S) (Figure 19).[53] The amine substituents can access both the buried waters (W) and the hydrophobic clamp (H), serving as a ring-opened version of the pyridylpyrazole in **5**.

In the second patent from Glenmark, WO2011/132051, inhibitor binding most likely occurs to the conserved glutamine (G) and the hydrophobic clamp via the methoxybenzofuran core (Figure 20).[54] The attached pyrrolodinone can occupy the ribose region with the pendent *N*-benzyl substituent reaching out to the exo-binding site (E). Data regarding selectivity over PDE4 are presented as a ratio (PDE4 IC_{50})/(PDE10A IC_{50}), which is not surprising considering the structural similarity to the PDE4 inhibitor rolipram.[55−57]

In the third patent from Glenmark, WO2011/138657, the 2-quinolylmethyloxy group is again used to fill the selectivity pocket (S) with an alkene helping to position key groups toward

dx.doi.org/10.1021/jm3004976 | J. Med. Chem. 2012, 55, 7299−7331

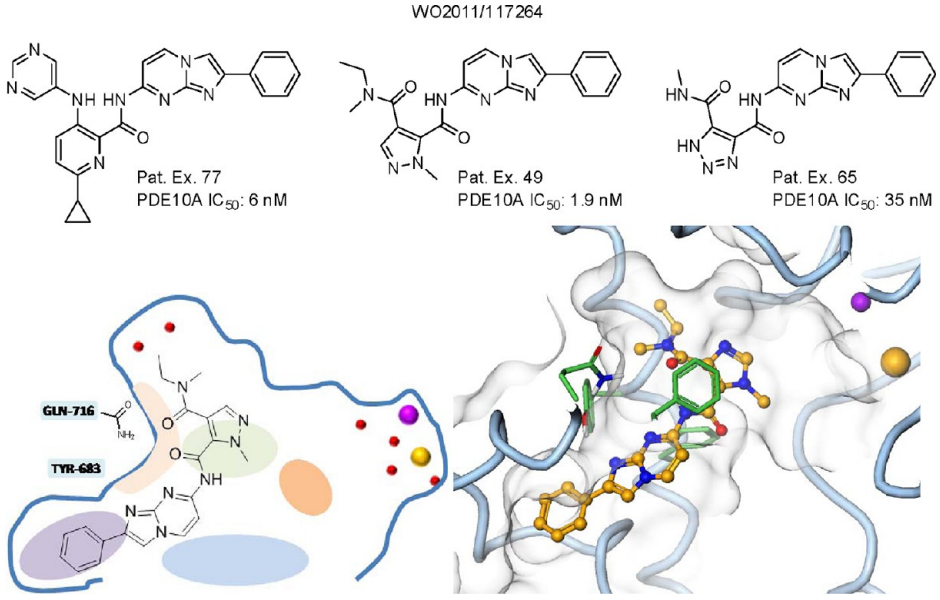

Figure 26. Examples of Hoffman-La Roche PDE10A inhibitors and a 2D and 3D representation of their proposed binding mode.

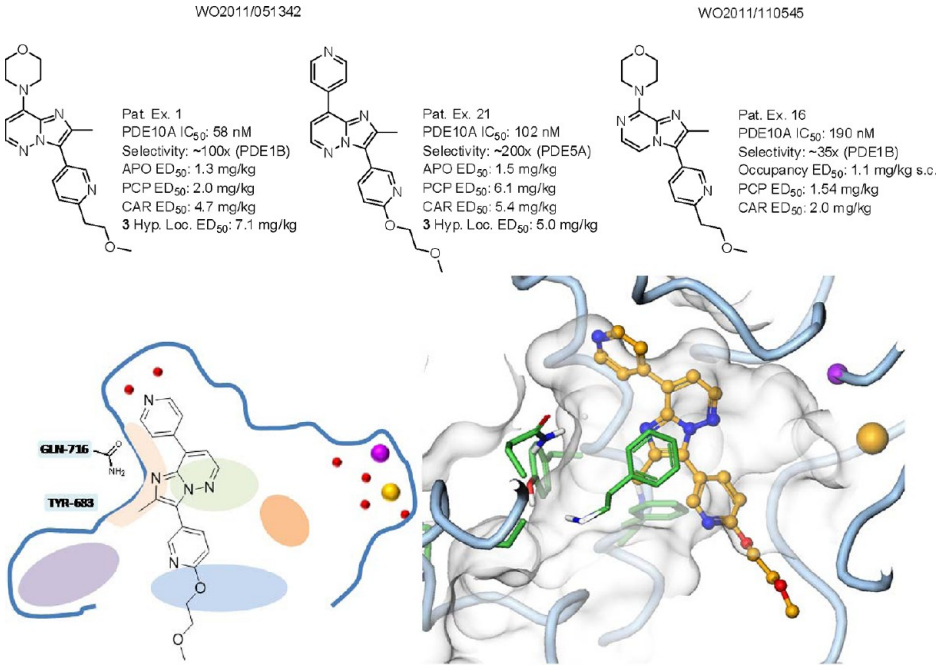

Figure 27. Highlighted Janssen compounds with biological activity and a 2D and 3D representation of the proposed binding mode.

the buried waters (W) and hydrophobic clamp (H).[58] Both compounds shown in Figure 21 were highlighted as demonstrating in vivo reversal of the effects of **2** in rat.

Hoffmann-La Roche. In 2010, Hoffmann-La Roche disclosed two patents that cover a series of pyrazolopyridazinone PDE10A inhibitors (Figure 22). The first patent[59] describes *N*-phenylpyridazinones with potency to 1 nM. The second patent[60] describes the *N*-heteroarylpyridazinones with IC_{50} < 10 nM. The SAR holds the pyrazolopyridazinone as a constant; therefore, it is these elements of the inhibitors that seem crucial for binding. There is no selectivity or in vivo data associated with these patents. In the absence of selectivity data, we have little confidence in proposing potential binding modes.

2011 has provided four more patent disclosures of potent PDE10A inhibitors from the Hoffmann-La Roche team. The first of these patents[61] describes many <1 nM K_i or IC_{50} inhibitors of PDE10A (Figure 23). There are no selectivity data associated with these inhibitors, but a modeling exercise can provide one possible binding mode where the phenyl substituted imidazopyridine can utilize the selectivity pocket with the nonbridgehead nitrogen anchoring the ligand through the Tyr H-bond. Additionally, with the methylpyrazole in the hydrophobic clamp, the two amide carbonyls can make a bidentate H-bond interaction with the invariant Gln.

The second 2011 disclosure of PDE10A inhibitors from Hoffmann-La Roche describes many potent inhibitors (<1 nM) with no selectivity or in vivo data (Figure 24).[62] Docking attempts suggest a pyridine or isoquinoline group occupying the selectivity pocket with a pyrazole or thiazole amide linker to the central pyridine ring which interacts with the invariant Gln.

dx.doi.org/10.1021/jm3004976 | J. Med. Chem. 2012, 55, 7299−7331

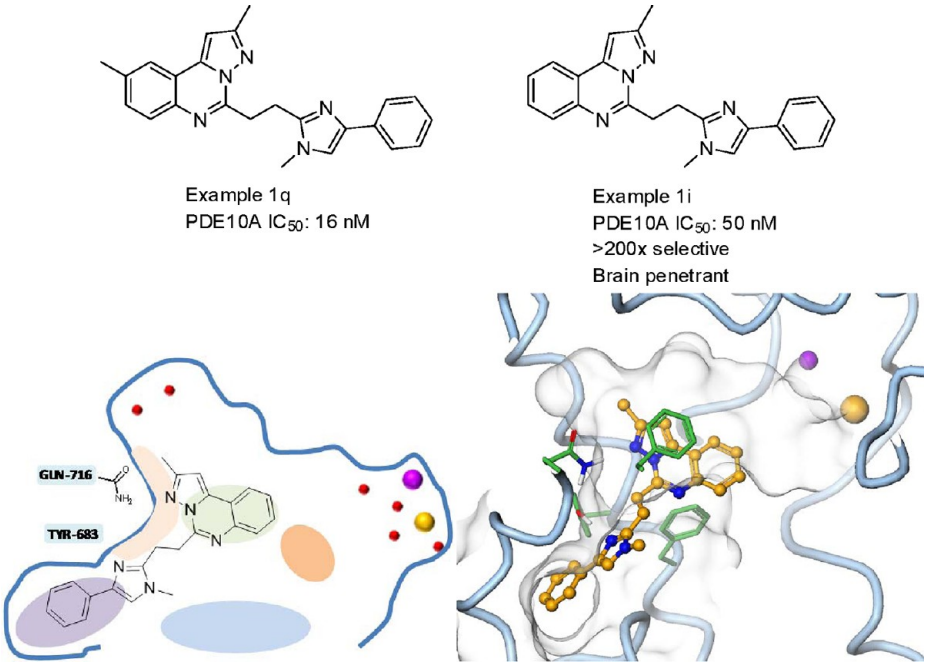

Figure 28. Examples of Lundbeck PDE10A inhibitors and a 2D and 3D representation of their proposed binding mode.

A recent patent application (WO2011/154327) by Hoffman-La Roche is quite intriguing.[63] They are able to extend the pendent N-linked pyrimidinecyclopropylheteroaryl series from more traditional selectivity pocket anchors such as quinoline and benzimidazoles to aryl groups with pendent amides. The interesting aspect of these new PDE10A inhibitors is that if these new inhibitors are binding similar to what we are proposing (Figure 25), these compounds would then be the first inhibitors to interact with the Tyr of the selectivity pocket with anything other than a heteroaryl H-bond acceptor.

A final 2011 installment in the expansion of this series of PDE10A inhibitors begins with the disclosure of a fused imidazopyrimidine with a pendent aryl group that presumably occupies the selectivity pocket.[63] This novel selectivity pocket group is then attached through an amide to the previously disclosed (Figure 24) cyclopyropylpyridine (example 77, Figure 26). This newly described selectivity pocket group is a sufficient anchor to allow the team to design significantly different rings, pyrazole and triazole, off the linker amide while still retaining significant PDE10A potency.

Janssen. Janssen has two new patent disclosures in 2011 of novel PDE10A inhibitors. Two examples of an imidazopyridazine series are highlighted below in Figure 27.[64] Example 1 is 58 nM vs PDE10A with ~100-fold selectivity vs PDE1B. Example 21 is 102 nM vs PDE10A and ~200-fold selective vs PDE5A. Given the moderate selectivities of these compounds vs other PDEs, it is likely that these compounds are not "selectivity pocket" inhibitors. They do have a rich rodent behavioral pharmacology package such as reversal of apomorphine induced stereotypy, reversal of PCP induced hyperlocomotion, conditioned avoidance response (CAR), reversal of **3** induced hypolocomotion (mice), and activity in novel object recognition. Docking, modeling, and SAR (lack of complete selectivity) combine to suggest that this imidazopyridazine series interacts with the invariant Gln while occupying the hydrophobic clamp. This provides a vector with which Janssen has appended a pyridine that can overlap the pyridyl of **5** (example 21, Figure 27). They are also able to use an N-linked morpholine as a suitable H-bond acceptor from the buried waters (W) of the enzyme. The other pyridyl appendage would therefore interact with the exo binding region of the enzyme. The second patent application is on a series of imidazopyrazines highlighted by example 16 (Figure 27) in WO2011/110545.[65] This compound is quite similar in activity in the primary enzyme assay, selectivity, and in vivo assays to the imidazopyridazine series that preceded it. And given the high similarity, the binding modes are presumably very similar.

Lundbeck. A significant amount of effort in developing novel PDE10A inhibitors has been disclosed over the past 2 years from Lundbeck. In 2010, the Lundbeck team disclosed a novel series of phenylimidazolpyrazoloquinazoline PDE10A inhibitors.[66] These inhibitors are able to utilize the "selectivity pocket" of PDE10A through an H-bond interaction between the Tyr and a nitrogen from the central imidazole ring, a slight but noticeable change from the fused heteroaryl acceptor moieties known previously. An ethylene spacer allows the fused tricyclic ring system to occupy the hydrophobic clamp region while interacting through a hydrogen bond to the invariant Gln through a nitrogen of the fused pyrazole. The most potent compound from this series is example 1q (Figure 28) at 16 nM vs PDE10A, but this compound had limited solubility and brain penetration. Example 1i drops off slightly in potency but allows for greater solubility and good brain penetration.

Lundbeck's 2011 publication describes a series of triazoloquinazolines that can inhibit PDE10A in several ways.[67] The fused triazoloquinazoline system occupies the hydrophobic clamp while making a hydrogen bond interaction with the invariant Gln. With a nitrile group off the thiomethylene linker, the inhibitor makes an additional interaction with a Ser in the back of the enzyme. While this motif did provide moderate potency (35 nM), these compounds had competing PDE4D activity. When the thiomethylene linker is attached to a fused benzimidazole, the inhibitor still occupies the hydrophobic clamp while making an

dx.doi.org/10.1021/jm3004976 | J. Med. Chem. 2012, 55, 7299−7331

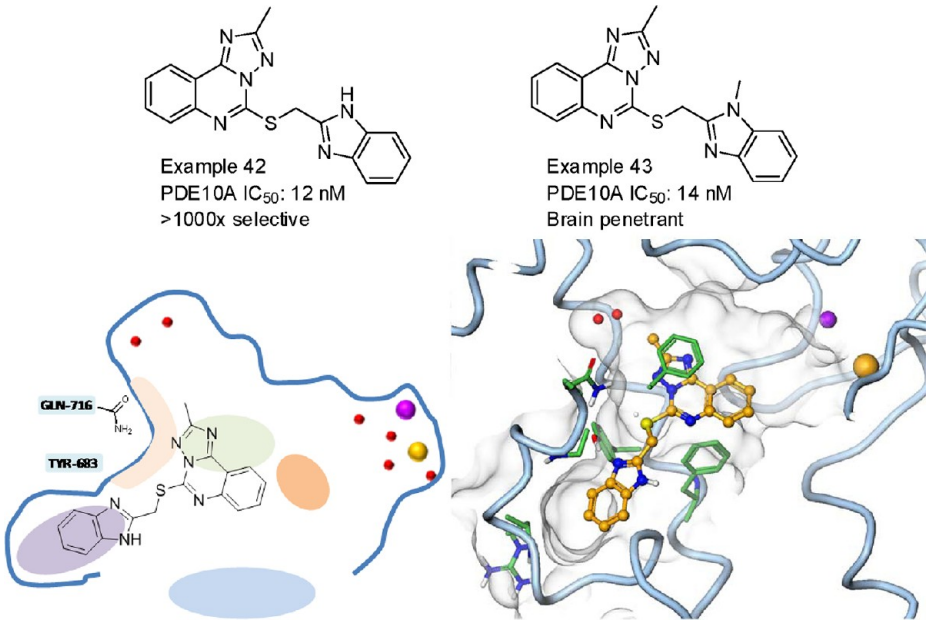

Figure 29. Highlighted examples from Lundbeck publication and a 2D and 3D representation of the binding mode (PDB entry 2Y0J).

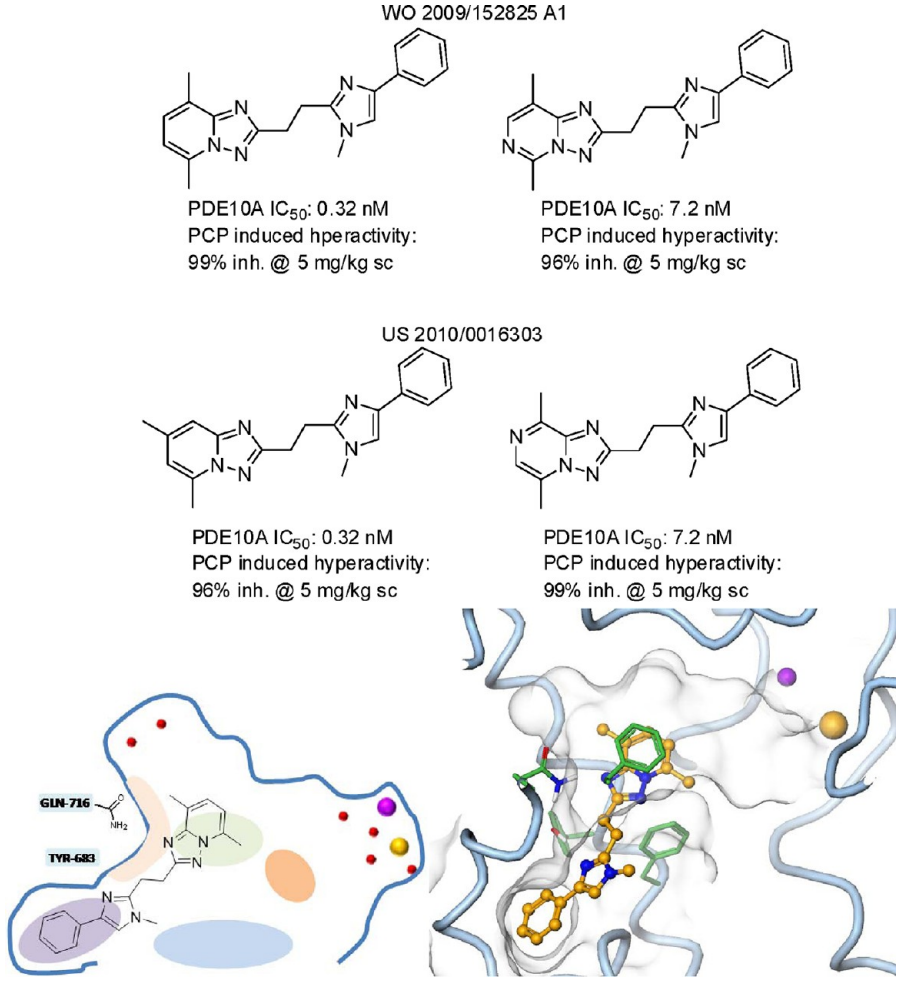

Figure 30. Examples of Lundbeck PDE10A inhibitors and a 2D and 3D representation of the proposed binding mode.

interaction with the invariant Gln but in a flipped mode that places the benzimidazole into the selectivity pocket. This combination of binding interactions allows for potency (12 nM) and selectivity (>1000×), example 42 (Figure 29). While the most potent compound had low brain penetration, a minor modification to the methylbenzimidazole substituent gave a

dx.doi.org/10.1021/jm3004976 | J. Med. Chem. 2012, 55, 7299−7331

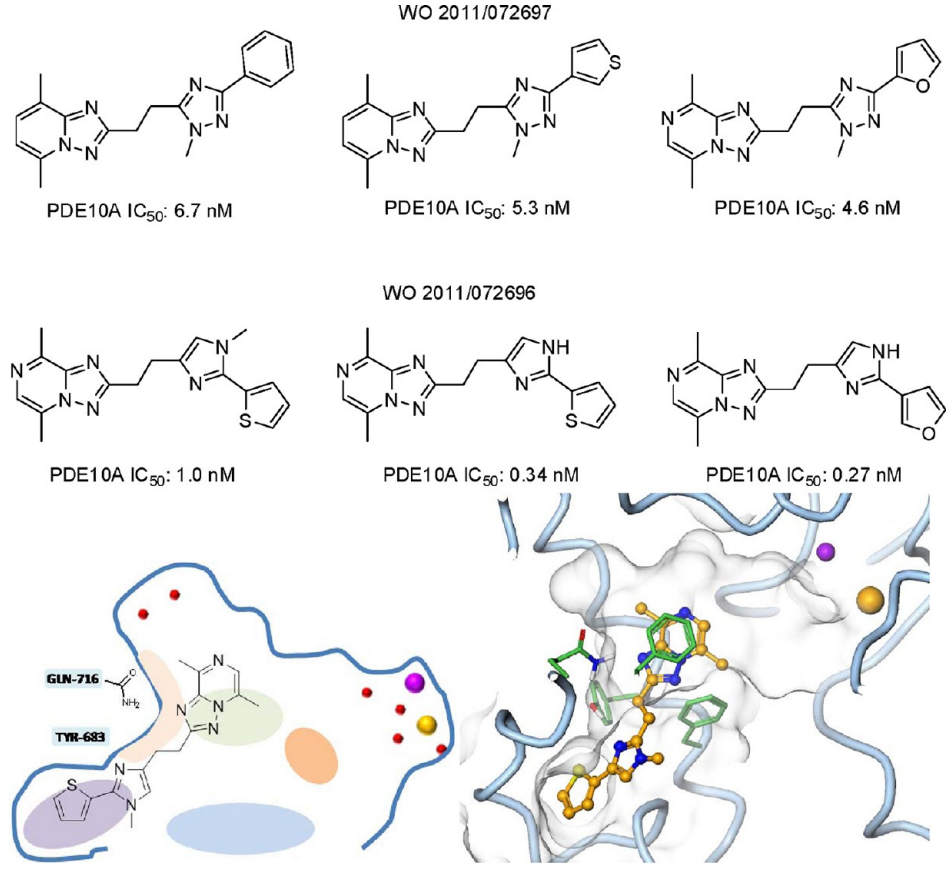

Figure 31. Examples from 2011 Lundbeck PDE10A patents and 2D and 3D representation of the proposed binding mode.

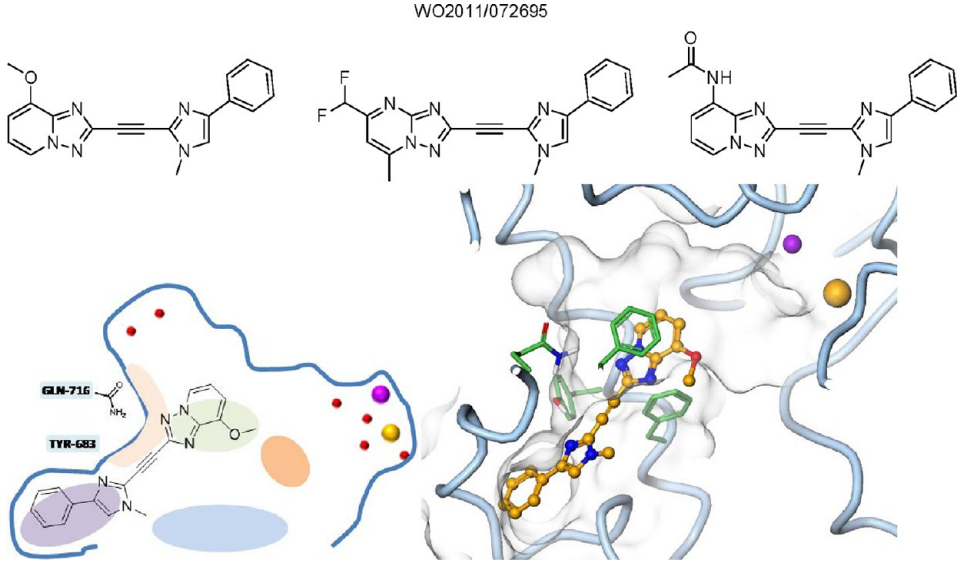

Figure 32. Examples from 2011 Lundbeck PDE10A patent and a 2D and 3D representation of their proposed binding mode.

negligent reduction in potency while allowing for high brain penetration, example 43 (Figure 29).

Some highlights from Lundbeck patents in 2009[68] and 2010[69] are shown in Figure 30 where compounds are described to have PDE10A potencies of <0.5 nM and potent in vivo activity measured by the reversal of PCP induced hyperactivity. Given the information that Lundbeck has provided in their publications, these compounds are certainly selectivity pocket binders.

Further expansion of Lundbeck's PDE10A chemical equity has provided two more patents describing very potent inhibitors. The first of these 2011 patents expands the scope of these previously disclosed series to include a triazole ring in place of the central imidazole.[70] Additionally, it shows that the pendent phenyl ring can easily be changed to accommodate a pendent heteroaryl ring and still retain all potency (Figure 31). The second 2011 PDE10A patent describes the scope and potency of the combination of the central imidazole

dx.doi.org/10.1021/jm3004976 | J. Med. Chem. 2012, 55, 7299−7331

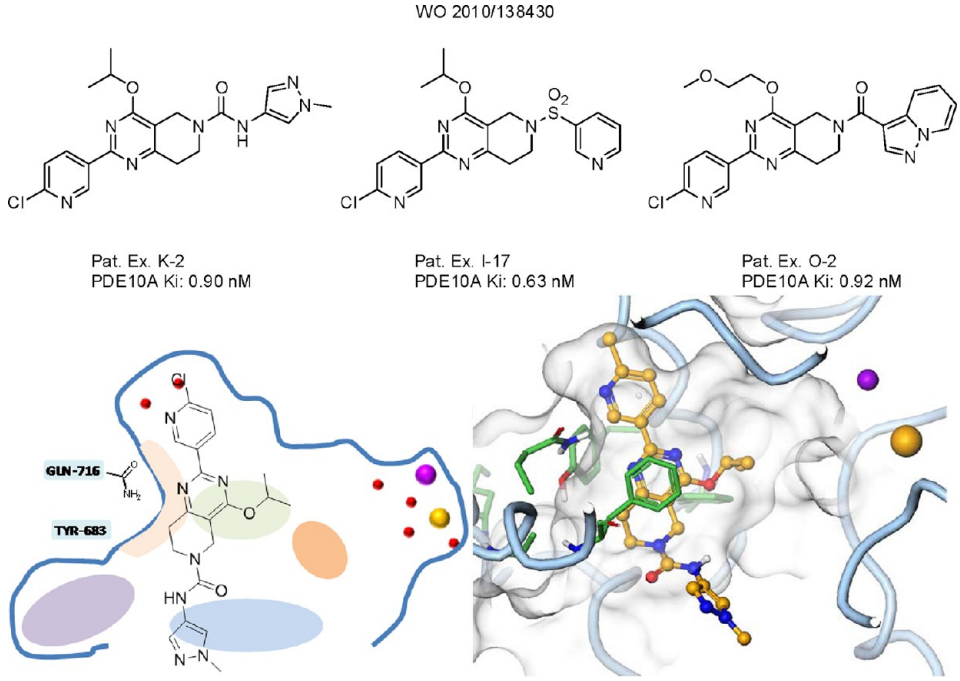

Figure 33. Examples of Merck PDE10A inhibitors and a 2D and 3D representation of the proposed binding modes.

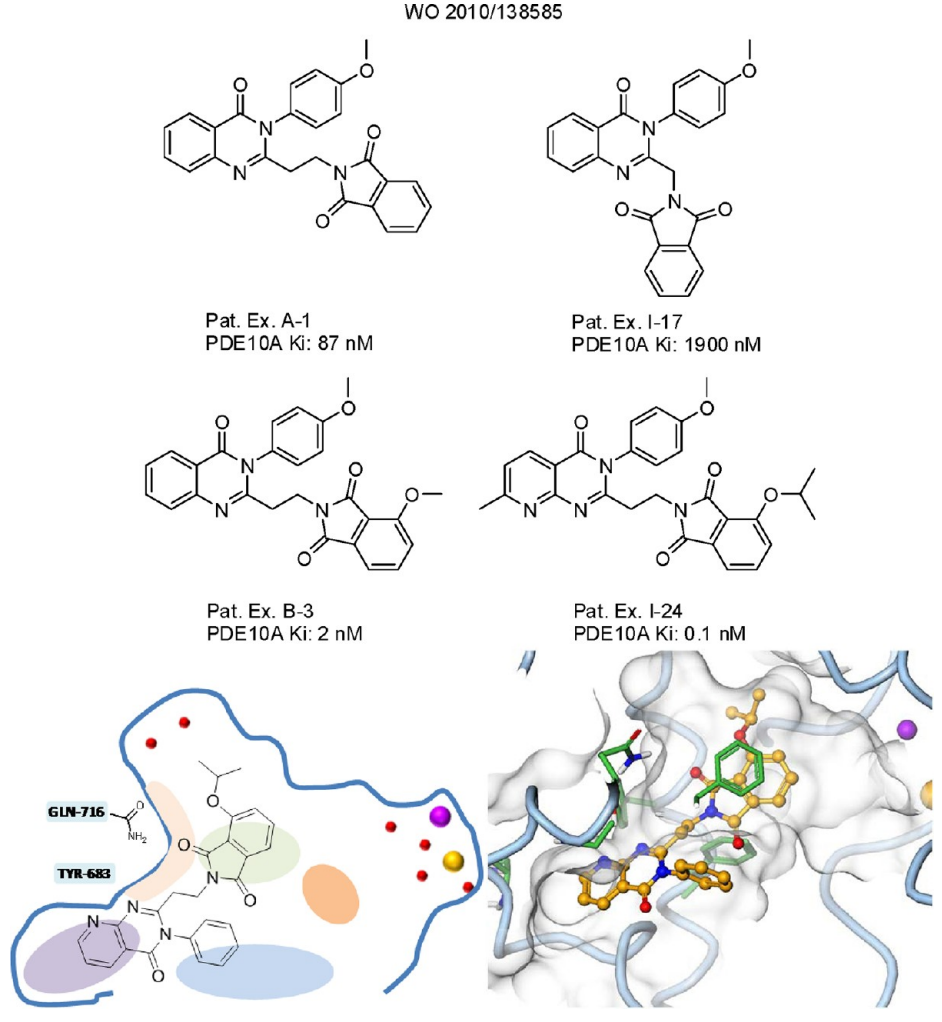

Figure 34. Examples of Merck PDE10A inhibitors and a 2D and 3D representation of the proposed binding modes.

dx.doi.org/10.1021/jm3004976 | J. Med. Chem. 2012, 55, 7299−7331

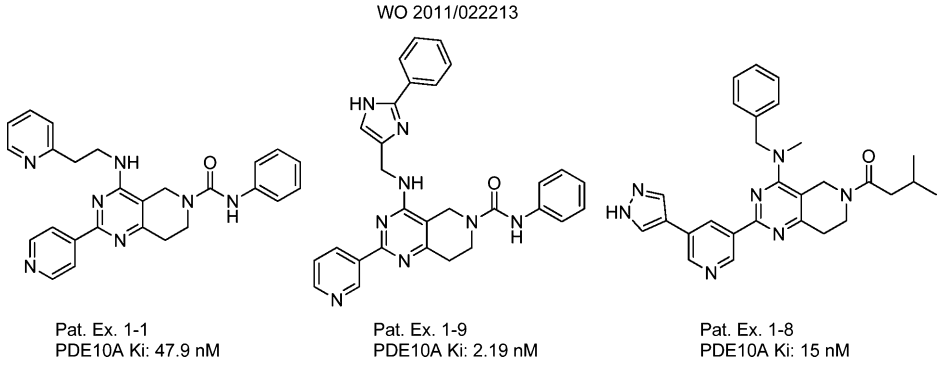

Figure 35. Representative examples of Merck PDE10A inhibitors.

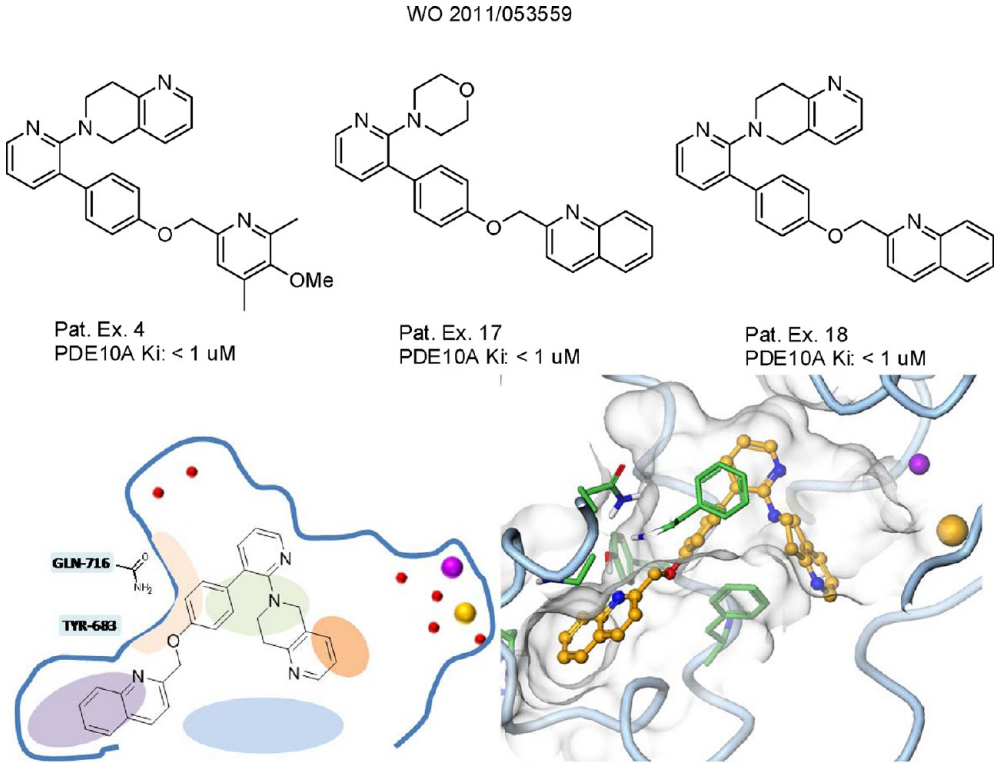

Figure 36. Examples of Merck PDE10A inhibitors and a 2D and 3D representation of the proposed binding modes.

ring and the pendent heteroaryl substituent.[71] The conversion back to the imidazole with the pendent heteroaryl ring gives ~5−10× more potency over the triazole comparator. This SAR provides a hint to the binding mode. If one of the nitrogens from the imidazole is making a key interaction with the enzyme, the loss in basicity/hydrogen bond acceptor strength in changing this ring to a triazole would account for the ~5−10× drop in potency.

A final 2011 PDE10A patent from Lundbeck describes a selectivity pocket anchor that is linked to the hydrophobic clamp heteroaryl moiety through an alkyne linker.[72] There is no PDE10A enzyme assay potency described in the patent. Some representative examples from the patent are provided in Figure 32.

Merck. Five unique series of PDE10A inhibitors have been patented by Merck, along with a potential PET ligand to help ascertain clinical target occupancy (see PET ligand section). WO2010/138430 describes inhibitors with a 4-alkoxy-5,6,7,8-tetrahydropyrido[4,3-*d*]pyrimidine core that have PDE10A K_i < 1 nM (Figure 33).[73] The 4-alkoxy group is generally a lower molecular weight aliphatic or alkoxy aliphatic. Substitution qon the piperidine is broad with amide, urea, sulfonamide, and heteroaryl being exemplified, while the attached pyridyl is generally 2-chloropyridine with a few cases of pyridine being shown. Binding to the invariant Gln-716 is predicted via the pyrimidine N-1 (G) which anchors the inhibitor. In docking of example K-2, the 2-chloropyridine fills the pocket containing the buried waters (W), potentially displacing these waters. The tetrahydropyridopyrimidine core sits in the hydrophobic clamp (H). The 4-alkoxy substituent appears to access the ribose region (R), and the piperidine amide points toward the exo-binding site (E).

In a series of patents disclosing *N*-arylquinazolines as ligands for PET imaging[74] (WO2010/138557) and related PDE10A inhibitors[75] (WO2010/138585) (Figure 34), exceptional potency is described (PDE10A K_i < 0.1 nM). The length of the carbon chain between the quinazoline and phthalimide is critical, with the two-carbon linker affording >20-fold

dx.doi.org/10.1021/jm3004976 | *J. Med. Chem.* 2012, 55, 7299−7331

more potency than the one-carbon linker. Substitution at the 3-position of the phthalimide is also important with the placement of methoxy (example B-3) being >40-fold more potent than the unsubstituted analogue (example A-1). Docking experiments suggest that the quinazoline binds in the selectivity pocket (S) with N-1 accepting a hydrogen bond from Tyr 683 while the *N*-aryl engages the exo-binding site (E). The flexible ethyl linker allows the phthalimide to simultaneously accept a hydrogen bond from Gln-716 via a carbonyl (G), occupy the hydrophobic clamp (H), and fill (W) with the isopropoxy group, which is consistent with the published SAR.

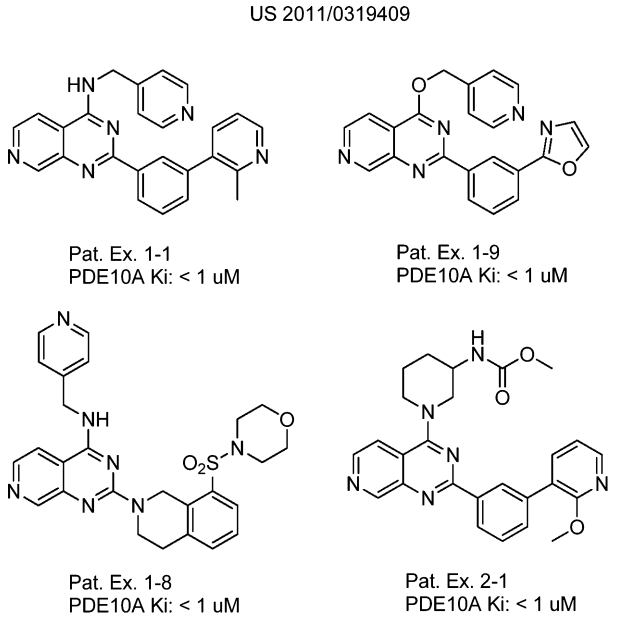

Figure 37. Representative examples of Merck PDE10A inhibitors.

4-Amino-5,6,7,8-tetrahydropyrido[4,3-*d*]pyrimidines disclosed in WO2011/022213[76] appear to be similar to the 4-alkoxy-5,6,7,8-tetrahydropyrido[4,3-*d*]pyrimidines in WO2010/138430 (see Figures 33 and 35). Key differences exist in disclosed SAR as larger amino substituents are described at the 4-position of the fused pyrimidinyl ring system than in the alkoxy-based patent. Additionally, heterocyclic substitution of the pyridyl ring is new and does not align with the previous SAR of this core. Attempted modeling of the SAR presented in the patent did not provide a single high scoring pose and may indicate multiple binding modes.

A series of aminopyridines is described in WO2011/053559 with stated K_i < 1 μM (Figure 36).[77] Side chains displaying 2-quinoline or 2-pyridine are present in several claimed compounds. This structural motif is reminiscent of that seen in

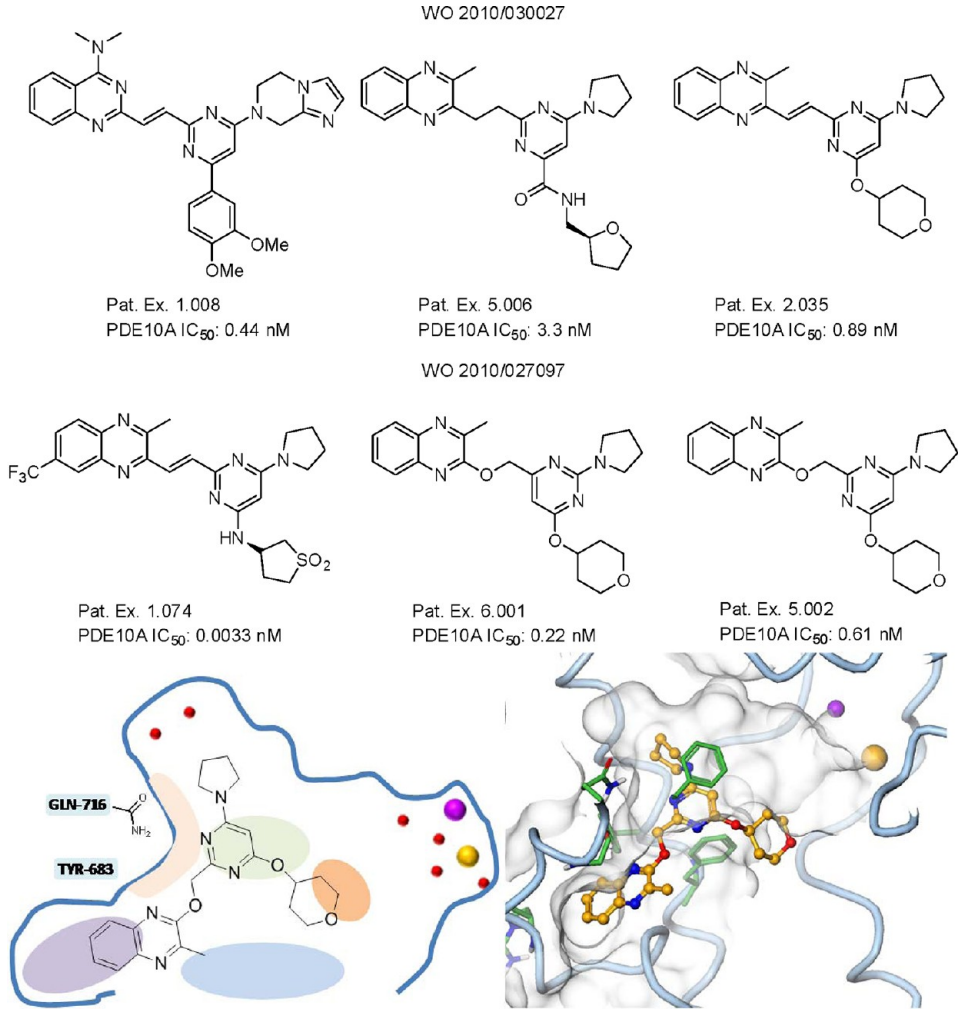

Figure 38. Examples of Mitsubishi-Tanabe PDE10A inhibitors from two patents and a 2D and 3D representation of the proposed binding mode.

dx.doi.org/10.1021/jm3004976 | *J. Med. Chem.* 2012, 55, 7299–7331

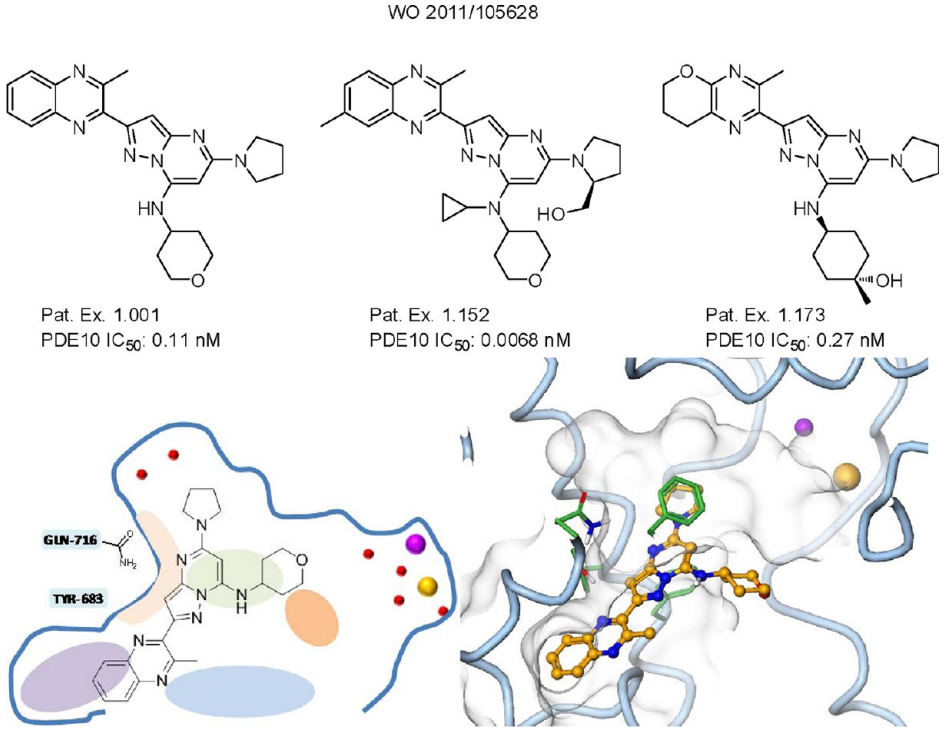

Figure 39. Examples of Mitsubishi-Tanabe PDE10A inhibitors and a 2D and 3D representation of the proposed binding mode.

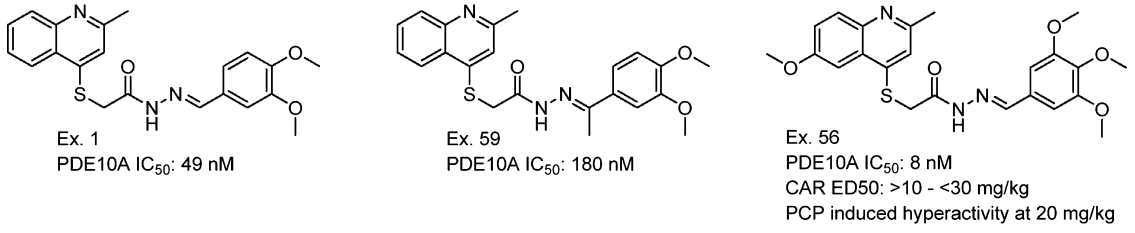

Figure 40. Examples of hydrazone PDE10A inhibitors disclosed by Omeros.

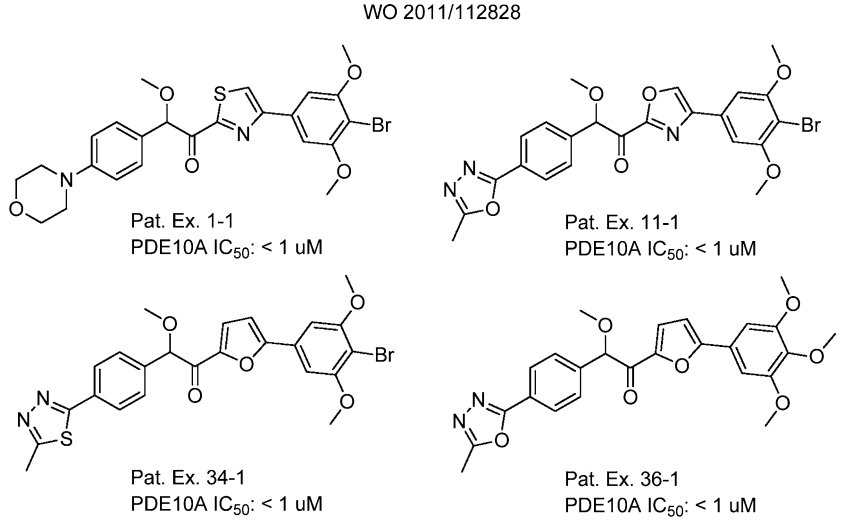

Figure 41. Examples of alkoxyarylacetyl PDE10A inhibitors from Omeros.

5 and most likely occupies the selectivity pocket (S) and accepts a hydrogen bond from Tyr 683 via the quinoline/pyridine nitrogen. In modeling example 18 from the patent, the alkoxyphenyl that is linked to the quinoline is aligned next to Gln-716 (G) and allows the centrally placed pyridine to occupy the buried water pocket (W). The aza-tetrahydroisoquinoline is positioned to fill the ribose pocket (R) and extend toward the waters surrounding the catalytic metals (M).

dx.doi.org/10.1021/jm3004976 | J. Med. Chem. 2012, 55, 7299−7331

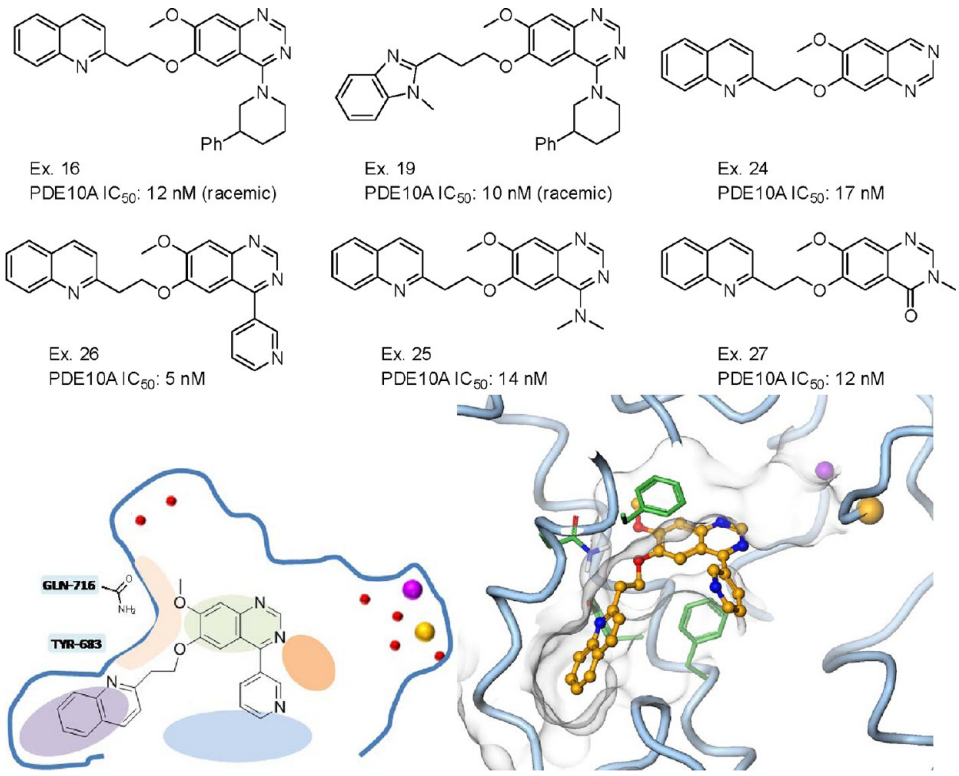

Figure 42. Examples from a 2011 paper by Pfizer of selective PDE10A inhibitors and a 2D and 3D representation of the binding mode.

A series of 5-azaquinazolines is disclosed in US2011/0319409 (Figure 37).[78] Lower molecular weight amines and ethers are exemplified at the 1-position of the quinazoline, whereas biaryl and tetrahydroisoquinoline substitution at the 3-position is exemplified.

Mitsubishi-Tanabe. Two patents from Mitsubishi-Tanabe, WO2010/030027 and WO2010/027097, disclose exceptionally potent PDE10A inhibitors (K_i < 1 nM) (Figure 38).[79,80] The most prevalent motif is of a quinazoline or quinoxaline that is attached to a disubstituted pyrimidine with a two-atom linker such as a trans double bond, an ethyl, or $-CH_2O-$. A proposed binding mode based on example 2.035 shows the quinoxaline simultaneously filling the selectivity pocket (S) while interacting with Tyr 683. A pyrimidine nitrogen accepts a hydrogen bond from Gln-716 (G). The pyrrolidine fits by the buried waters (W), while the more polar tetrahydropyran can reach the waters surrounding the catalytic metals (M).

A more rigid series of quinoxaline-based inhibitors is disclosed in WO2011/105628 wherein a fused bicyclic core replaces previous alkyl, alkenyl, and alkoxyalkyl linkers (Figure 39).[81] Similar amino groups are present on the pyrazolopyrimidine core as on the pyrimidine core previously published, suggesting similar binding modes. Exceptional potency is reported with IC_{50} values as low as 0.0068 nM.

Omeros. A very extensive analysis of a hydrazone series of PDE10A inhibitors was detailed in a 2011 paper by Omeros.[82] They describe the different SAR aspects of this series starting from a library hit (Ex. 1, Figure 40). The methylisoquinoline ring is not critical to PDE10A activity, as it can be changed to small aryl groups such as pyrimidine, pyridine, substituted phenyl, biphenyl, and naphthyl with loss of activity of up to ~10-fold. But the substituted methylisoquinoline is the most potent aryl that was presented. The sulfur linker could be replaced by oxygen or nitrogen but with loss of potency. Various substitutions on or around the hydrazone were tolerated without significant loss of potency, although a 3-fold loss of potency resulted through the addition of a methyl group between the hydrazone and the pendent phenyl ring. This is presumably due to a change in the population of the geometry of the most potent form of the inhibitor (Ex. 59, Figure 40). The description of the pendent phenyl group SAR is limited to a di- or trimethoxy group. There is no X-ray structural information within the paper. If the potency is truly limited to methoxy substituents on this aryl ring, it would lead us to presume that this series is binding to the invariant Gln in a bidentate interaction, much like the early PDE10A catechol based inhibitors. Because of the considerable flexibility of the hydrazone-thiomethylene linker, modeling efforts to further interrogate the other possible PDE10A enzymatic interactions provided too many plausible options. Selectivity of this series is described as being 110- to >1250-fold selective over all other PDEs.

α-Alkoxyarylacetyl derivatives in WO2011/112828 are claimed to have PDE10A IC_{50} < 1 μM (Figure 41).[83] In vivo efficacy of these compounds in mouse in reversing the effects of PCP in a locomotor assay and preventing conditioned avoidance responding is presented. The binding mode to PDE10A is not clear, although the presence of the arylalkoxy groups suggests potential interaction with the conserved glutamine as in the dimethoxycatechols like **6** and papaverine.

Pfizer. In a 2011 paper Pfizer reported on a series of selective quinazolines and quinazolinones that were discovered utilizing structure-based design and ligand efficiency to merge to distinct chemical series (Figure 42).[33] The quinazoline/quinazolinone core occupies the hydrophobic clamp (H) with pendent alkoxy groups binding to the conserved glutamine (G). Building off the 6-alkoxy with both ethyl and propyl linkers and into the selectivity pocket with quinoline and benzimidazole affords both potency and selectivity. Significant SAR flexibility is observed

dx.doi.org/10.1021/jm3004976 | J. Med. Chem. 2012, 55, 7299−7331

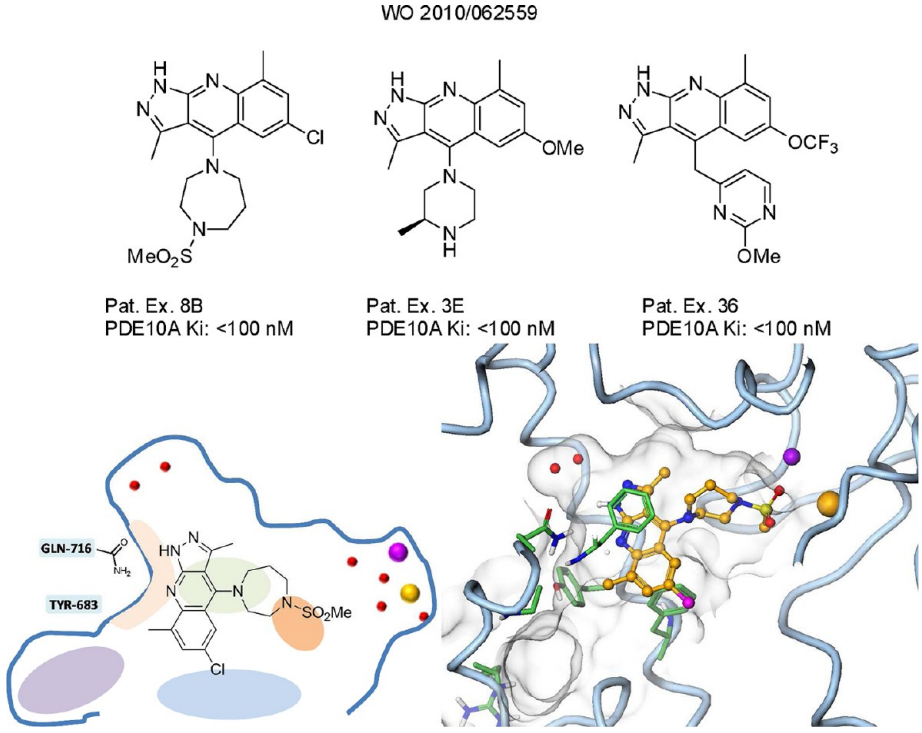

Figure 43. Representative examples of Schering-Plough PDE10A inhibitors and 2D and 3D binding modes (modeled based on PDB entry 3UI7).

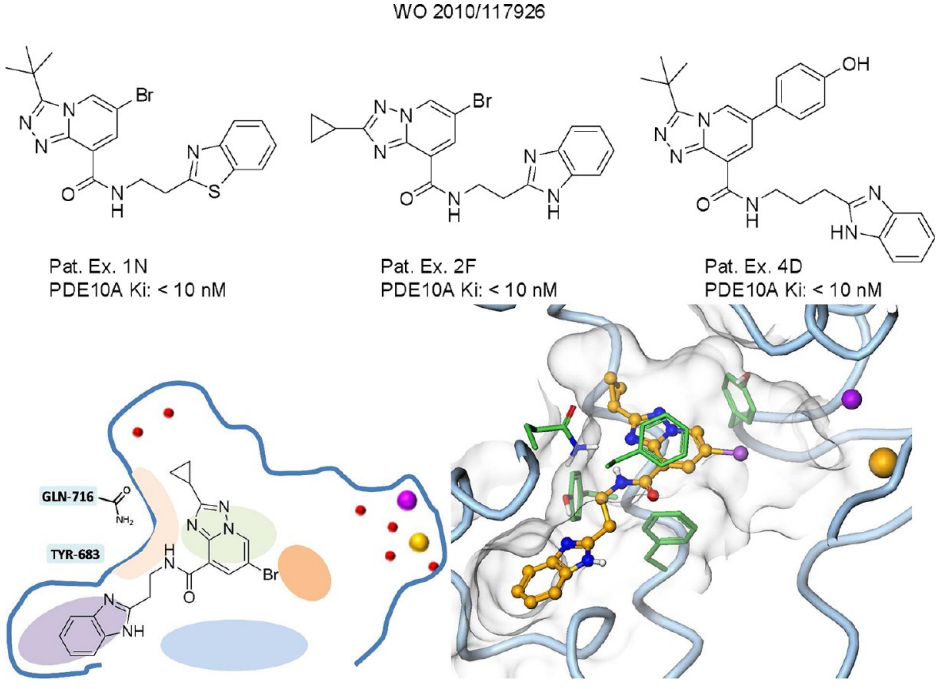

Figure 44. Examples of Schering-Plough PDE10A inhibitors and a 2D and 3D representation of the proposed binding mode.

building off the 4-position of the quinazoline, pointing toward the exo-binding site (E), where amines and heteroaryl rings are tolerated, thus allowing for modulation of ADME properties. In vivo activity in CAR and increases in brain cGMP are reported.

Schering-Plough. The Schering-Plough organization published two patents in 2010 and one in 2011, covering a variety of inhibitor structural classes. The first patent, WO2010/062559, disclosed a series of pyrazoloquinolines.[84] Modeling efforts did not identify a single binding mode that appeared to explain the disclosed SAR, and thus, none is suggested. It is noted that significant diversity is tolerated on the 4-position of the quinoline (e.g., diazapine, piperazine, CH_2-pyrimidine), suggesting that this vector could be pointing toward the exo-binding site (E) or the metals (M). The relative invariance of the aryl ring substitution pattern with an ortho-methyl and para group may indicate key hydrophobic interactions. Manual docking of example 8B was carried out, with the assumption that the pyrazolo NH and quinoline N interact with Gln-716 and that the

dx.doi.org/10.1021/jm3004976 | J. Med. Chem. 2012, 55, 7299−7331

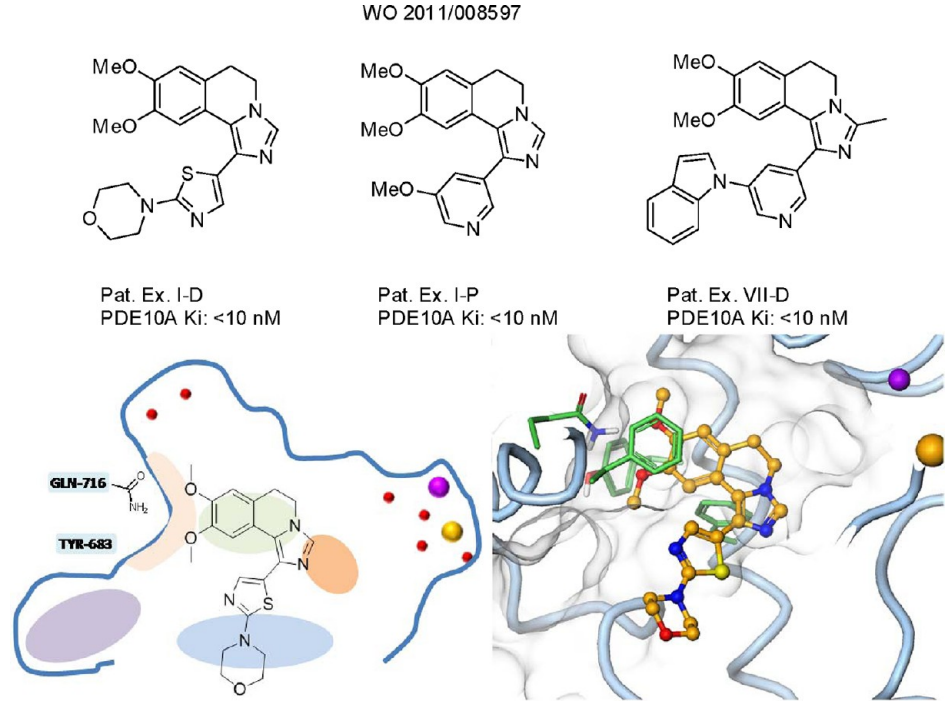

Figure 45. Examples of Schering-Plough PDE10A inhibitors and a 2D and 3D representation of the proposed binding mode.

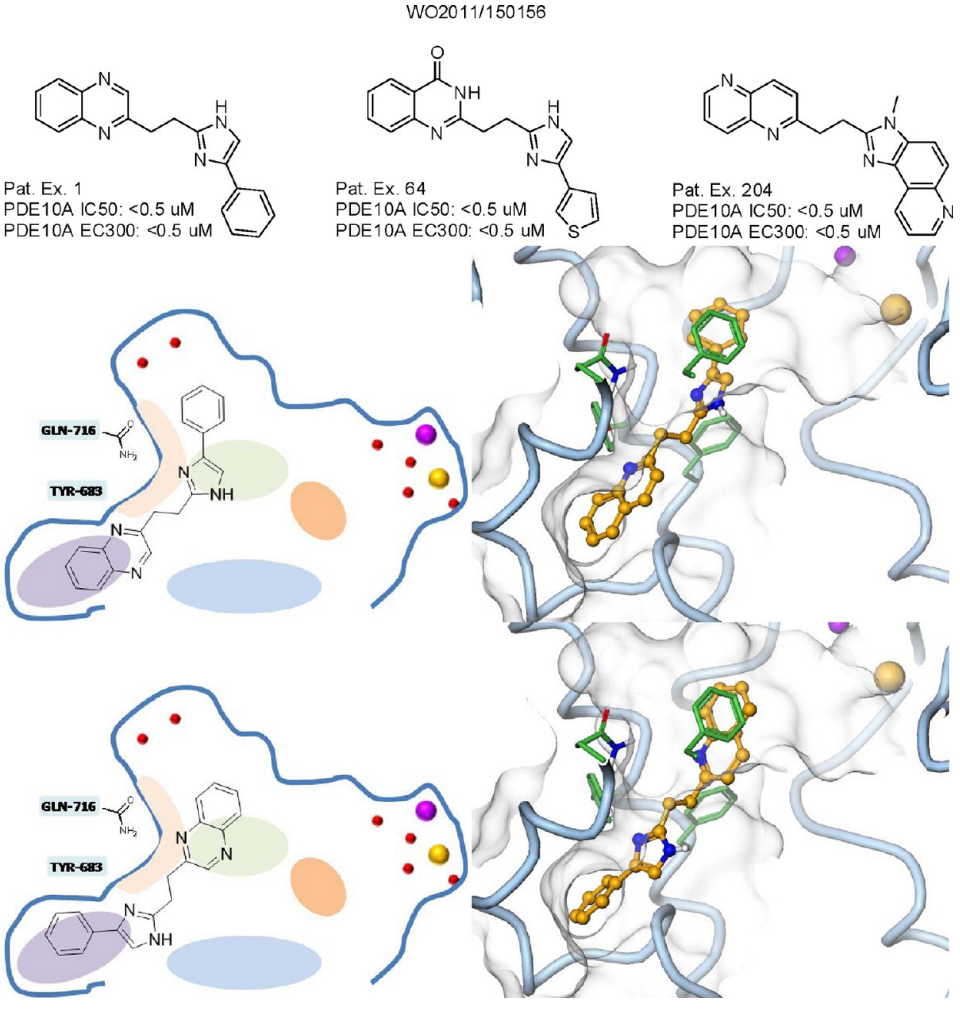

Figure 46. Examples of Sunovion PDE10A inhibitors and the 2D and 3D representations of the two proposed binding modes.

dx.doi.org/10.1021/jm3004976 | J. Med. Chem. 2012, 55, 7299−7331

tricyclic ring system occupies the hydrophobic clamp (H). Two different orientations are possible for the fused substituted phenyl ring with it positioned to the front of the binding pocket or to the back. A very recent publication, however, verifies the docking pose shown in Figure 43.[85]

In the second published patent, WO2010/117926, PDE10A K_i < 10 nM is reported for a series of fused triazolopyridines with differing relative positions of the triazole nitrogens and the pendent carbon substituent (Figure 44).[86] An amide group is constant with the amide side chain being a two- to three-carbon linker attached to a fused [6,5] heterocycle, such as benzimidazole or benzthiazole. Docking example 2F into the PDE10A X-ray structure showed that the triazolopyridine filled the hydrophobic clamp (H). The pendent amide carbonyl (bolded) accepted a hydrogen bond from GLN-716 (G). The benzimidazole filled the selectivity pocket (S), and benzimidazole nitrogen accepted a hydrogen bond from Tyr-683 at the entrance to the pocket. Cyclopropyl filled the pocket containing the buried waters (W). The bromine atom sits under the hydrophobic clamp and is pointed toward the metals. The SAR in example 4D (4-phenol for bromo) is suggestive of additional hydrogen bonding interactions with the waters surrounding the metals (M).

In the third patent, WO2011/008597, a dimethoxytetrahydroisoquinoline motif with a fused imidazole was reported.[87] Significant SAR of the imidazole 4-position is observed with a variety of substituted heterocycles showing potent activity. Computational modeling of example 1-D (Figure 45) suggested a binding mode similar to the dimethoxyquinazolines papaverine and **6**. The dimethoxy group formed a bidentate hydrogen bond with the Gln-716 (G), and the tricyclic imidazotetrahydroisoquinoline filled the hydrophobic clamp (H). The morpholinothiazole projected into the exo-binding site (E), which was experimentally supported by a broad SAR at this position.

Sunovion. The chemistry team at Sunovion has put together an impressive array of PDE10A inhibitors that expand on the well precedented theme of anchoring inhibitors into the selectivity pocket and then linking to a heteroaryl group that can occupy the hydrophobic clamp and at the same time interacting through a hydrogen bond interaction with the invariant glutamine. This ensures an inhibitor that is selective and relatively potent. Additionally, they have identified that both of these themes (heteroaryl groups that make H-bonds to the enzyme) are the same. Thus, they have attached known selectivity pocket anchors

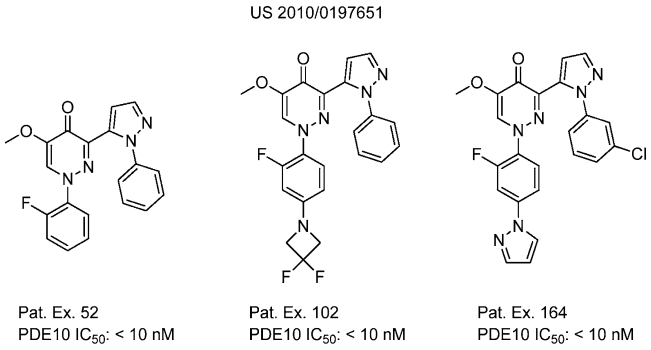

Figure 47. Representative examples of Takeda PDE10A inhibitors.

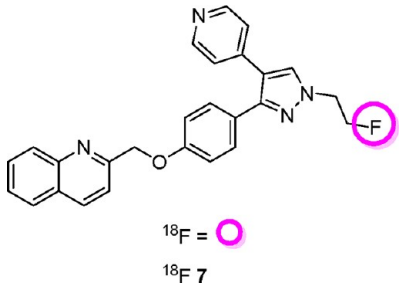

Figure 49. PDE10A PET ligand ^{18}F **7**.

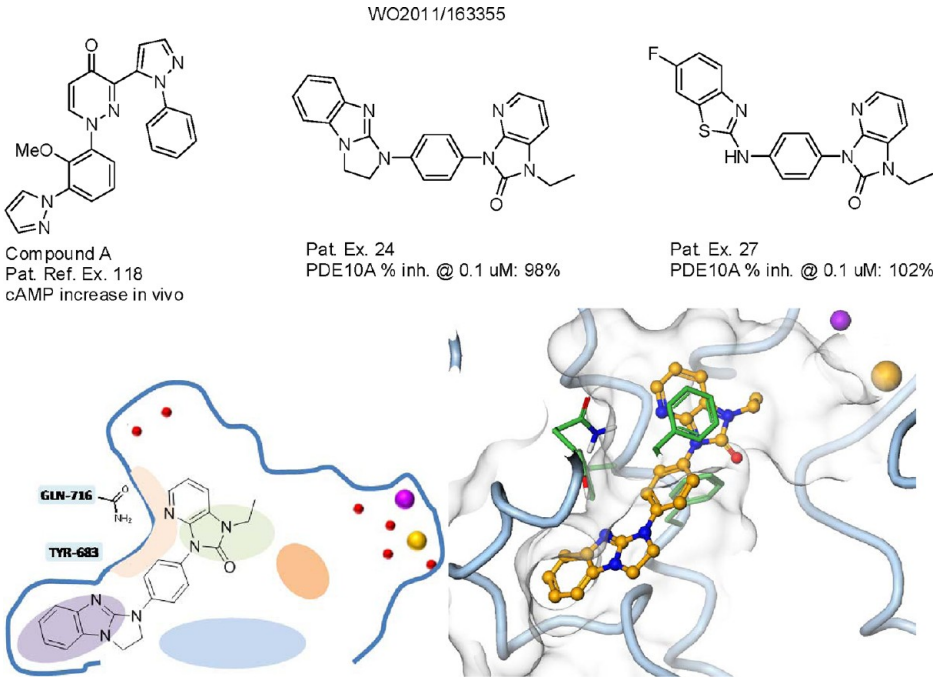

Figure 48. Examples of Takeda PDE10A inhibitors and a 2D and 3D representation of the proposed binding mode.

dx.doi.org/10.1021/jm3004976 | J. Med. Chem. 2012, 55, 7299–7331

to both ends of an ethylene linker (Figure 46, Pat. Ex. 1 and Pat. Ex. 64). This ensures that the selectivity pocket is occupied. Sunovion seems to be the first company to disclose the use of a whole cell assay as a functional measure of activity.[88] On top of the primary binding assay, they describe a whole cell assay in which HEK293 cells overexpress PDE10A. In these cells the inhibitor concentration in which the intracellular cAMP concentration is increased by 300% is used to generate an EC_{300}. Exact numbers are not disclosed, but the company describes 31 compounds with $IC_{50} < 0.5\ \mu M$ in the primary binding assay and $EC_{300} < 0.5\ \mu M$ in the whole cell assay.

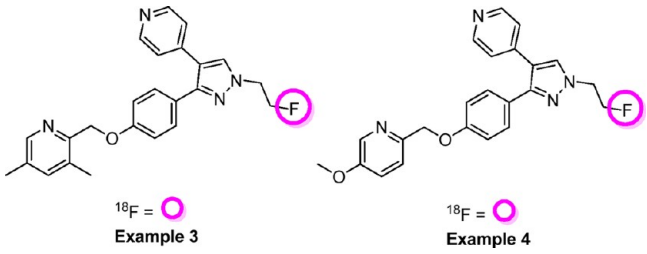

Figure 50. Highlighted examples of new PDE10A PET ligands.

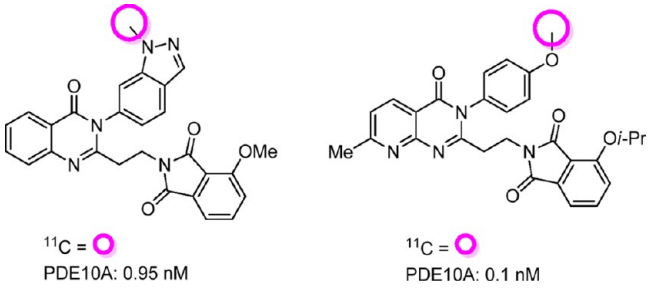

Figure 51. Merck PDE10A PET ligand examples.

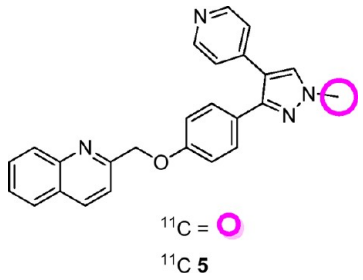

Figure 52. Washington University generated ^{11}C **5**.

Takeda. Takeda discloses 1-aryl-5-methoxy-3-(1-aryl-1*H*-pyrazol-5-yl)pyridazin-4(1*H*)-ones (Figure 47) as PDE10A inhibitors that are claimed to increase striatal cGMP, inhibit both **2** and amphetamine increases in LMA, and increase **2**-induced PPI.[89] This class of compounds is similar to a series patented by scientists at Hoffman-La Roche. Automated docking to PDE10A provided a wide variety of potential binding poses, thus making it difficult to suggest a favored inhibitory motif. Key observations in the SAR are relative invariance of the pyridazinone core and attached arylpyrazole wherein a simple phenyl is primarily exemplified. In contrast, the pyridazinone *N*-1-aryl tolerates significant variety in the groups attached, suggesting that this group may extend into the exo-binding site (E).

A follow-up patent from Takeda expands on the pyridizanone series where the methoxy next to the central carbonyl has been removed.[90] Compound A (Pat. Ex. 118, Figure 48) is accompanied by data showing in vivo cAMP increases. Interestingly, the Takeda scientists have also included a novel series of PDE10A inhibitors within this patent. These new imidazopyridinone inhibitors can be modeled with a heteroaromatic "selectivity pocket" anchor, a phenyl spacer, and an imidazopyridinone to occupy the hydrophobic clamp and simultaneously accept a hydrogen bond from the invariant Gln. These compounds, Pat. Ex. 24 and Pat. Ex. 27 (Figure 48), are potent and presumably quite selective, although a PDE10A IC_{50} is not presented.

PET LIGANDS

There is a growing interest in the development of positron emission tomography (PET) imaging of PDE10A inhibitors. PET ligands most commonly have ^{11}C or ^{18}F incorporated into the radionucleotide in the final step of synthesis as the agent for emitting the γ rays that are being detected. PET is a useful tool for drugs that target the CNS, as it is a noninvasive measure of drug disposition, localization, and quantification in both preclinical species and humans. It is possible to displace the PET ligand

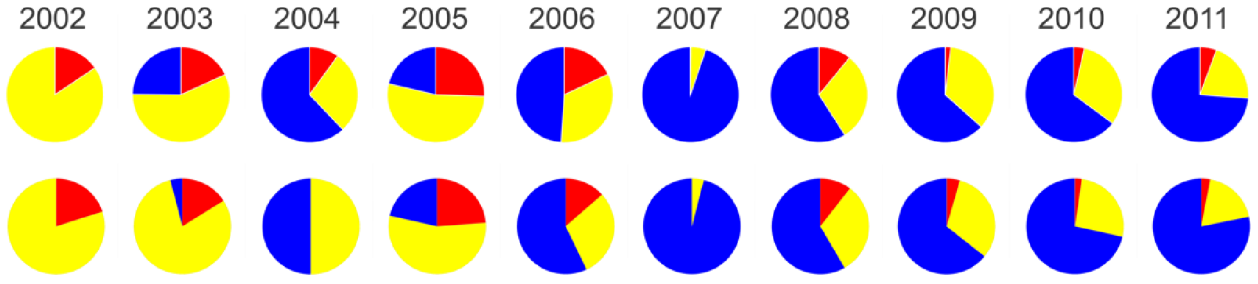

Figure 53. Top row: CNS MPO score of exemplified patented PDE10A inhibitors over time. Bottom row: CNS MPO scores of 20 random structures from each PDE10A patent.

Table 3. Analysis of the Number of Companies Patenting PDE10A Inhibitors, the Number of PDE10A Patents Filed, and the Number of Novel Murko Graph Frameworks with at Least Five Exemplified Structures

	2002	2003	2004	2005	2006	2007	2008	2009	2010	2011
no. of companies	1	1	1	2	4	4	4	7	13	10
no. of patents	1	2	3	2	5	9	3	12	20	22
no. of unique frameworks	3	6	1	4	29	20	20	12	62	87

dx.doi.org/10.1021/jm3004976 | *J. Med. Chem.* 2012, 55, 7299–7331

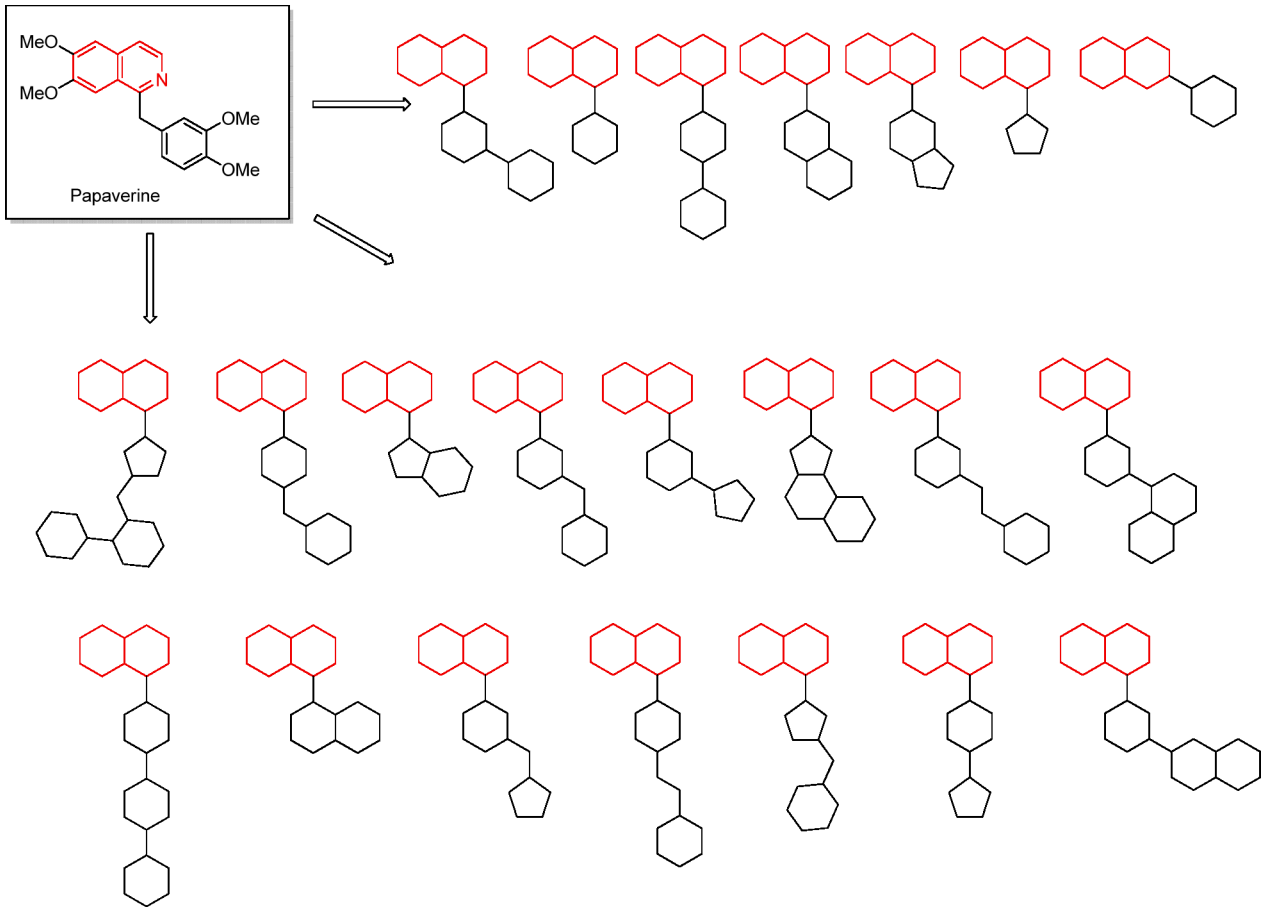

Figure 54. Murko frameworks from two or more companies whose genesis may come from the first disclosed PDE10A inhibitor papaverine. Highlighted in red are the common structural features.

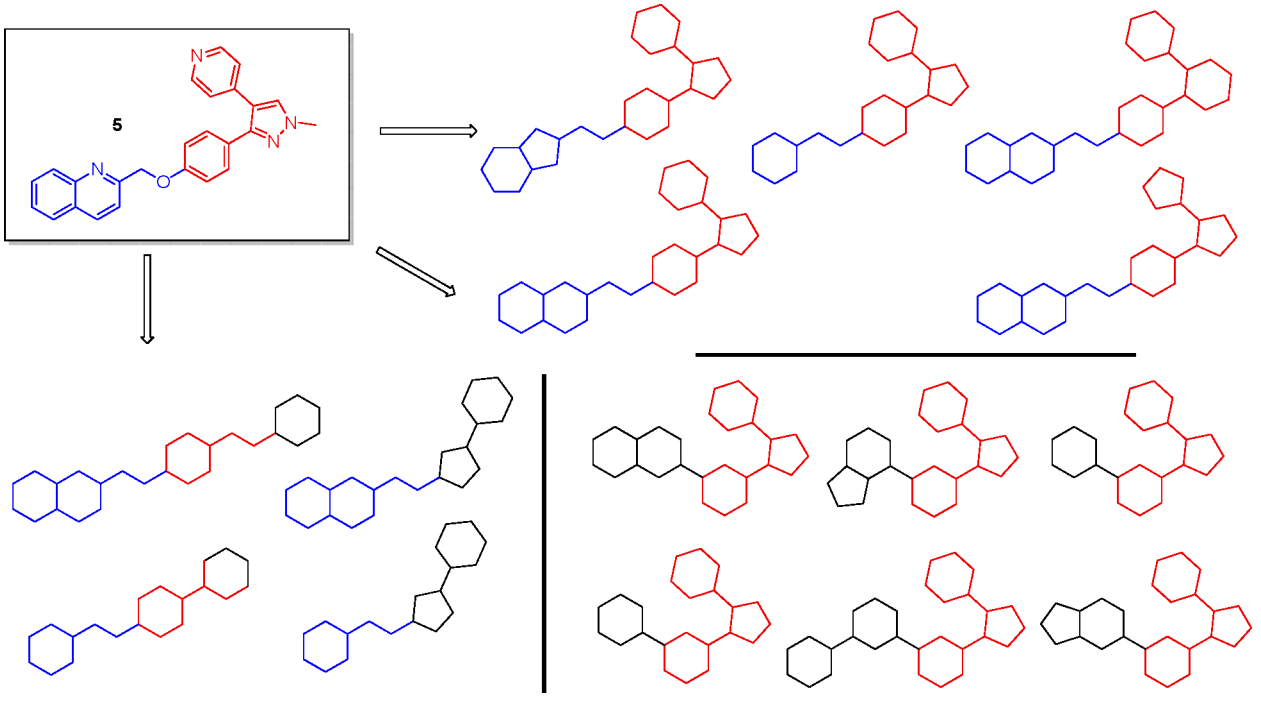

Figure 55. Murko frameworks from two or more companies with their origin being **5**. Highlighted in red and blue are the common structural features.

with the desired drug, accurately assess the degree of enzyme engagement, and correlate this with preclinical target engagement data at efficacious plasma concentrations to ensure the optimal doses for assessing clinical efficacy.[91] Given several publications

dx.doi.org/10.1021/jm3004976 | J. Med. Chem. 2012, 55, 7299−7331

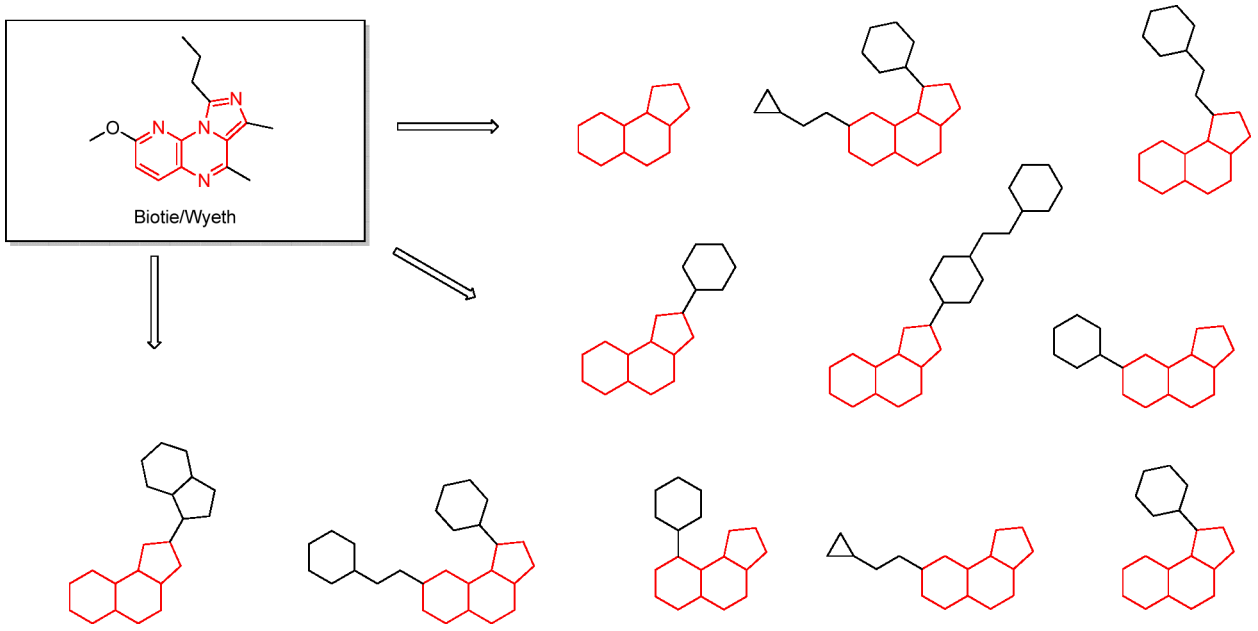

Figure 56. Murko frameworks from two or more companies with their origin in Biotie/Wyeth inhibitors. Highlighted in red are the common structural features.

and patents for PDE10A PET ligands within the past several years, it is reasonable to imagine that companies are preparing for or have already begun to move PDE10A inhibitors into the clinic.

Johnson and Johnson. A full preclinical evaluation of an ^{18}F analogue of **5**, **7** (JNJ41510417), was disclosed in 2010 (Figure 49).[92] This compound is highly potent and selective and was found to have high CNS penetration and reversibly binds to PDE10A. PDE10A knockout mice were used to determine that the binding to mouse brain is attributed solely to PDE10A.

Janssen. Janssen set out to optimize the ^{18}F-JNJ41510417 PET ligand by designing into the new ligands better PET physicochemical properties than their starting point, **5**.[93,94] They were able to identify two new potential ligands, example 3 and example 4 (Figure 50). A side by side in vivo evaluation showed both compounds to be potent, selective, brain penetrant compounds. Example 3 proves to be the better compound because of good brain uptake, accumulation, and higher signal to background properties.

Merck. Merck has extended one of their PDE10A inhibitor series into potential PET ligands.[74] These compounds are very potent with activity (K_i) to 0.02 nM. Two examples from this patent are represented in Figure 51.

Washington University. Researchers at Washington University School of Medicine evaluated ^{11}C **5** (Figure 52) as a PET ligand in mice and rhesus monkeys.[95] Non-human primate PET studies clearly show a high uptake of ^{11}C **5** into the striatum, particularly the putamen and caudate. Unfortunately, this team found that a radiolabeled brain penetrant metabolite may limit the use of this ligand as a PET tracer in the clinic.

■ ANALYSES OF PDE10A INHIBITOR PROPERTY AND CHEMICAL SPACES

Given that PDE10A is mainly localized to the striatal area of the brain and PDE10A inhibitors are designed to target neurological diseases, we wanted to analyze PDE10A inhibitors of the patent literature for their overall chemical diversity, druglikeness, and ability to access the CNS compartment. Exemplified patent structures of PDE10A patents through 2011 were collected based on IBM Patent Analytic Platform.[96]

The CNS multiple parameter optimization (MPO) desirability tool was based on six fundamental molecular properties and was shown to be a superior druglikeness factor for CNS drugs.[97] We felt that the best way to measure this was through collections of the exemplified compounds in all PDE10A patents through 2011 and then to analyze their CNS MPO desirability score trend. The CNS MPO score is binned into three categories: 0−3 (low, red), 3−4 (medium, yellow), 4−6 (high, blue). More than 75% of marketed CNS drugs possess CNS MPO scores of 4 and above. A high CNS MPO score was shown to lead to a higher probability in alignments of ADME/T, specifically CNS

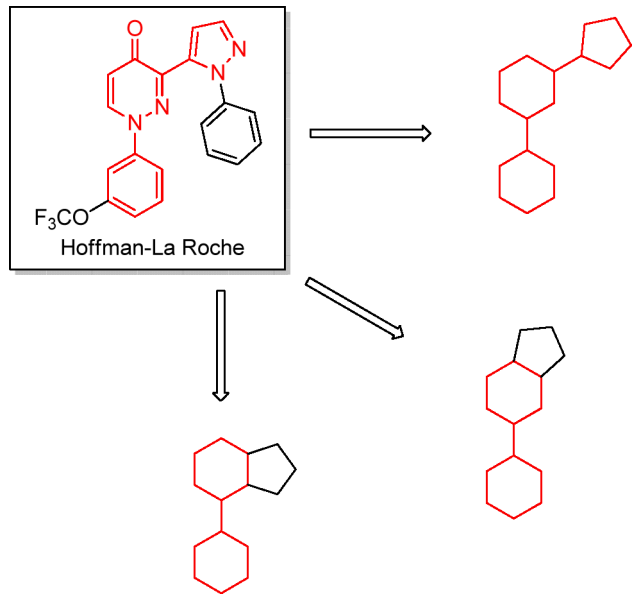

Figure 57. Murko frameworks from two or more companies with their origin from compounds like those disclosed from Hoffman-La Roche. Highlighted in red are the common structural features.

dx.doi.org/10.1021/jm3004976 | J. Med. Chem. 2012, 55, 7299−7331

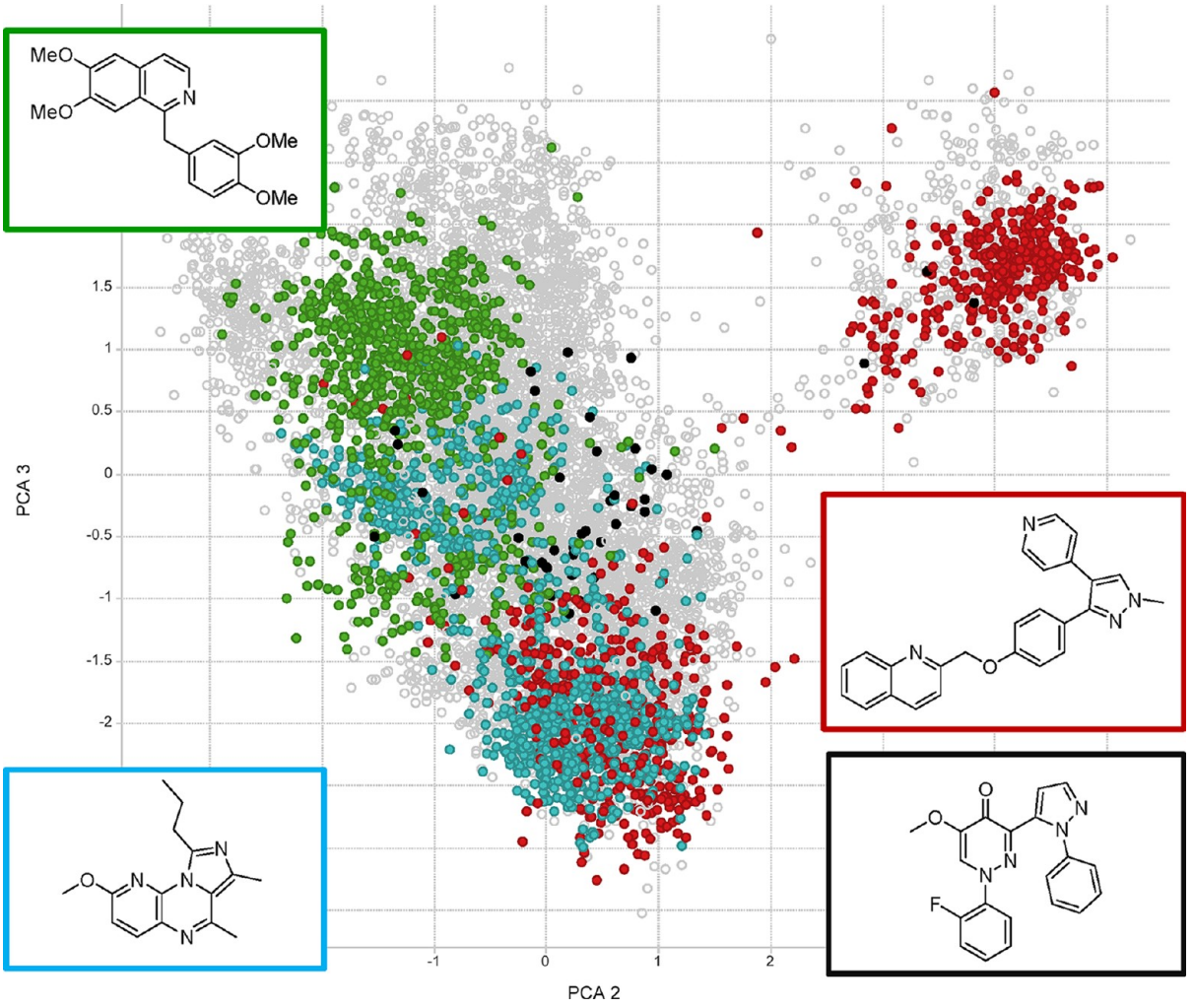

Figure 58. Principal component analysis of patent exemplified PDE10A inhibitors. Solid circle represents structures containing one of the Murcko frameworks worked on by two or more companies, as shown in Figures 54−57. Opened circle represents the rest of the exemplified structures. Solid dots are color-coded by framework families. Green is for families associated with papaverine. Red is for families associated with **5**. Blue is for Biotie-Wyeth family, and black is for Roche−Takeda family.

permeability, clearance, and safety. Figure 53 shows the CNS MPO scores of all patent exemplified PDE10A inhibitors extracted from the IBM patent database over time. The top pie chart of Figure 53 is a representation of the CNS MPO score of all exemplified patented PDE10A inhibitor compounds. In an attempt to prevent overrepresentation of property space by patents with a large number of exemplified structures, a normalized set of up to 20 random exemplified compounds from each patent was also generated. The CNS MPO profile of this set is nearly identical to that of the full set as shown in the bottom pie charts of Figure 53. An improvement trend of CNS MPO distribution demonstrated the medicinal chemistry effort through the industry toward more druglikeness compounds.

Since the first patent in 2002, the interest in PDE10A has expanded rapidly within the biomedical community. A peak of 13 different companies filed patents in 2010, while a peak in the number of filed patents (22) was in the most recent year of analysis, 2011 (Table 3). Murcko graph framework[98] demonstrated a high diversity within the PDE10A patent space. A significant increase in the number of unique and novel Murcko graph frameworks has occurred within the past 2 years.

Additional insight could also be revealed through analyses of the most common Murcko frameworks that have appeared in patents from two or more companies. We found that the majority of the Murko frameworks could be traced back to a handful of unique starting points. The majority of the Murko frameworks traced back to the first disclosed PDE10A inhibitor, papaverine (Figure 54). **5** has also led to a significant amount of follow-up (Figure 55) by other companies. Biotie/Wyeth (Figure 56) type compounds were popular starting points for the generation of PDE10A inhibitors. Lastly, there is a series of compounds exemplified by Hoffman-LaRoche and Takeda that is being investigated by those two companies (Figure 57).

The interweaving relationship of frameworks, chemical diversity, and key recognition features specific to PDE10A could be demonstrated through principal component analysis. A principal component analysis (PCA) is a linear projection method to visualize high dimensional space in lower dimensions.[99] The ECFP4 fingerprints[100] were generated for all exemplified patent structures, and principal components were generated with the TIBCO SpotFire package.[101] As shown in Figure 58, while only 30% of all patent exemplified structures were embodied in the frameworks shown in Figures 54−57, the four "families" of Murcko graph frameworks span most of the chemical space occupied by all exemplified structures, indicating additional common chemical features and molecular recognition elements

dx.doi.org/10.1021/jm3004976 | J. Med. Chem. 2012, 55, 7299−7331

between the frameworks. This is a testament to the creativity of the medicinal chemists that are working in this arena to the high druggability of the PDE10A enzyme.

CONCLUSION

Our developing understanding of the preclinical biological consequences of PDE10A inhibition continues to point to PDE10A inhibition having a beneficial role most notably in diseases such as schizophrenia and Huntington's, although other diseases may well be impacted through this mechanism of action. The design of inhibitors of PDE10A has been guided from the beginning by X-ray cocrystallographic information. The greatest impact of the structural knowledge of PDE10A was the disclosure of the "selectivity pocket" by **5**. The impact of this is clearly seen over the past several years through the patent literature. An analysis of the past several years' patents and publications leads us to believe that the vast majority of new inhibitors are taking advantage of the selectivity and potency gained through this particular design element. Additionally, brain penetration is not perceived to be an issue with many companies disclosing compounds that have high CNS MPO scores. As such, one might expect to soon see a large number of potent and highly selective PDE10A inhibitors that achieve CNS penetration, testing the PDE10A inhibition hypothesis in the clinic, close behind the active clinical candidate **5**.

AUTHOR INFORMATION

Corresponding Author

*Phone: 617-395-0712. E-mail:Thomas.a.chappie@pfizer.com.

Notes

The authors declare no competing financial interest.

Biographies

Thomas A. Chappie is a Senior Principal Scientist in the Department of Neuroscience Medicinal Chemistry at Pfizer, Inc. His focus during the past 10 years has been almost exclusively in the field of phosphodiesterases. He has been a member of several teams that have designed and developed brain penetrant phosphodiesterase inhibitors that have advanced into the clinic. In 2004 he was acknowledged by the American Chemical Society as a "Rising Star in Industrial Research" (Young Industry Investigators Forum) and in 2009 with the "Technical Achievement Award" from the Organic Chemistry Division of the American Chemical Society. He holds B.S. and M.S. degrees from Ohio University (1990 and 1993).

Christopher J. Helal is Senior Director in Neuroscience Medicinal Chemistry in Groton, CT. During his time at Pfizer (1997 to present) he has engaged medicinal chemistry efforts across a range of targets, in particular identification of brain penetrant, subtype selective phosphodiesterase (PDE) inhibitors, leading to the identification of several clinical candidates. He has also engaged in the effective utilization of parallel chemical synthesis to drive the hit-to-lead process. He received his B.S. degree in Chemistry at the Ohio State University (1987–1991) and carried out his doctoral studies at Harvard University, MA (1991–1997), with Nobel Laureate Professor Elias J. Corey, where he expanded the scope of the enantioselective oxazaborolidine-catalyzed (CBS) reduction of ketones and developed a number of highly efficient and enantioselective syntheses of pharmaceutical agents.

Xinjun Hou is currently Associate Research Fellow and the Head of Neuroscience Computational Chemistry of Pfizer Worldwide Research and Development in Cambridge, MA. He joined the Computational Chemistry Group of Agouron Pharmaceutical, Inc., now part of Pfizer Worldwide R&D, in 1992 to develop novel computational techniques to advance structure-based drug design. Xinjun has contributed to computational strategies such as structure-based drug design, HTS triaging, virtual screening, and in silico ADMET modeling through his career at Agouron and Pfizer. His computational modeling efforts directly impacted the discovery of clinical candidates targeting PDE10A, PDE9A, GlyT1, and AMPA receptor. Xinjun received his B.S. in Physics at Peking University, China, and earned his M.S. in Computer Sciences and Ph.D. in Physics from Drexel University in Philadelphia, PA.

ABBREVIATIONS USED

GAF, cGMP-stimulated PDE, *Anabaena* adenylyl cyclase, and the *Escherichia coli* transcription factor FhIA; CREB, cAMP response element binding protein; CAR, conditioned avoidance response; SLA, spontaneous locomotor activity; PCP, phencyclidine; AMPH, amphetamine; D_1, dopamine receptor subtype 1; D_2, dopamine receptor subtype 2; CRE, cAMP response element; H_3, histone receptor subtype 3; siRNA, small interfering ribonucleic acid; MPO, multiple parameter optimization

REFERENCES

(1) Loughney, K.; Snyder, P. B.; Uher, L.; Rosman, G. J.; Ferguson, K.; Florio, V. A. Isolation and characterization of PDE10A, a novel human 3′,5′-cyclic nucleotide phosphodiesterase. *Gene* **1999**, *234*, 109–117.

(2) Fujishige, K.; Kotera, J.; Omori, K. Striatum- and testis-specific phosphodiesterase PDE10A. *Eur. J. Biochem.* **1999**, *266*, 1118–1127.

(3) Fujishige, K.; Kotera, J.; Michibata, H.; Yuasa, K.; Takebayashi, S.; Okumura, K.; Omori, K. Cloning and characterization of a novel human phosphodiesterase that hydrolyzes both cAMP and cGMP (PDE10A). *J. Biol. Chem.* **1999**, *274*, 18438–18445.

(4) Soderling, S. H.; Bayuga, S. J.; Beavo, J. A. Isolation and characterization of a dual-substrate phosphodiesterase gene family: PDE10A. *Proc. Natl. Acad. Sci. U.S.A.* **1999**, *96*, 7071–7076.

(5) Adamowicz, W.; Bove, S.; Romegialli, A.; Mariga, A.; Kleiman, R. In *Society for Neuroscience*; San Diego, CA, 2010.

(6) Lakics, V.; Karran, E. H.; Boess, F. G. Quantitative comparison of phosphodiesterase mRNA distribution in human brain and peripheral tissues. *Neuropharmacology* **2010**, *59*, 367–374.

(7) Seeger, T. F.; Bartlett, B.; Coskran, T. M.; Culp, J. S.; James, L. C.; Krull, D. L.; Lanfear, J.; Ryan, A. M.; Schmidt, C. J.; Strick, C. A.; Varghese, A. H.; Williams, R. D.; Wylie, P. G.; Menniti, F. S. Immunohistochemical localization of PDE10A in the rat brain. *Brain Res.* **2003**, *985*, 113–126.

(8) Coskran, T. M.; Morton, D.; Menniti, F. S.; Adamowicz, W. O.; Kleiman, R. J.; Ryan, A. M.; Strick, C. A.; Schmidt, C. J.; Stephenson, D. T. Immunohistochemical localization of phosphodiesterase 10A in multiple mammalian species. *J. Histochem. Cytochem.* **2006**, *54*, 1205–1213.

(9) Kotera, J.; Fujishige, K.; Yuasa, K.; Omori, K. Characterization and phosphorylation of PDE10A2, a novel alternative splice variant of human phosphodiesterase that hydrolyzes cAMP and cGMP. *Biochem. Biophys. Res. Commun.* **1999**, *261*, 551–557.

(10) Kotera, J.; Sasaki, T.; Kobayashi, T.; Fujishige, K.; Yamashita, Y.; Omori, K. Subcellular localization of cyclic nucleotide phosphodiesterase type 10A variants, and alteration of the localization by cAMP-dependent protein kinase-dependent phosphorylation. *J. Biol. Chem.* **2004**, *279*, 4366–4375.

(11) Charych, E. I.; Jiang, L.-X.; Lo, F.; Sullivan, K.; Brandon, N. J. Interplay of palmitoylation and phosphorylation in the trafficking and localization of phosphodiesterase 10A: implications for the treatment of schizophrenia. *J. Neurosci.* **2010**, *30*, 9027–9037.

(12) Matthiesen, K.; Nielsen, J. Binding of cyclic nucleotides to phosphodiesterase 10A and 11A GAF domains does not stimulate catalytic activity. *Biochem. J.* **2009**, *423*, 401–409.

(13) Heikaus, C. C.; Pandit, J.; Klevit, R. E. Cyclic Nucleotide binding GAF domains from phosphodiesterases: structural and mechanistic insights. *Structure* **2009**, *17*, 1551−1557.
(14) Schmidt, C. J.; Chapin, D. S.; Cianfrogna, J.; Corman, M. L.; Hajos, M.; Harms, J. F.; Hoffman, W. E.; Lebel, L. A.; McCarthy, S. A.; Nelson, F. R.; Proulx-LaFrance, C.; Majchrzak, M. J.; Ramirez, A. D.; Schmidt, K.; Seymour, P. A.; Siuciak, J. A.; Tingley, F. D., III; Williams, R. D.; Verhoest, P. R.; Menniti, F. S. Preclinical characterization of selective phosphodiesterase 10A inhibitors: a new therapeutic approach to the treatment of schizophrenia. *J. Pharmacol. Exp. Ther.* **2008**, *325*, 681−690.
(15) Clineschmidt, B. V.; Martin, G. E.; Bunting, P. R. Anticonvulsant activity of (+)-5-methyl-10,11-dihydro-5*H*-dibenzo[*a*,*d*]cyclohepten-5,10-imine (MK-801), a substance with potent anticonvulsant, central sympathomimetic, and apparent anxiolytic properties. *Drug Dev. Res.* **1982**, *2*, 123−134.
(16) Clineschmidt, B. V.; Martin, G. E.; Bunting, P. R.; Papp, N. L. Central sympathomimetic activity of (+)-5-methyl-10,11-dihydro-5*H*-dibenzo[*a*,*d*]cyclohepten-5,10-imine (MK-801), a substance with potent anticonvulsant, central sympathomimetic, and apparent anxiolytic properties. *Drug Dev. Res.* **1982**, *2*, 135−145.
(17) Höfgen, N.; Stange, H.; Schindler, R.; Lankau, H.-J.; Grunwald, C.; Langen, B.; Egerland, U.; Tremmel, P.; Pangalos, M. N.; Marquis, K. L.; Hage, T.; Harrison, B. L.; Malamas, M. S.; Brandon, N. J.; Kronbach, T. Discovery of imidazo[1,5-*a*]pyrido[3,2-*e*]pyrazines as a new class of phosphodiesterase 10A inhibitiors. *J. Med. Chem.* **2010**, *53*, 4399−4411.
(18) Iorio, L. C.; Barnett, A.; Leitz, F. H.; Houser, V. P.; Korduba, C. A. SCH 23390, a potential benzazepine antipsychotic with unique interactions on dopaminergic systems. *J. Pharmacol. Exp. Ther.* **1983**, *226*, 462−468.
(19) Chappie, T.; Humphrey, J.; Menniti, F.; Schmidt, C. PDE10A inhibitors: an assessment of the current CNS drug discovery landscape. *Curr. Opin. Drug Discovery Dev.* **2009**, *12*, 458−467.
(20) Verhoest, P. R.; Chapin, D. S.; Corman, M.; Fonseca, K.; Harms, J. F.; Hou, X.; Marr, E. S.; Menniti, F. S.; Nelson, F.; O'Connor, R.; Pandit, J.; Proulx-LaFrance, C.; Schmidt, A. W.; Schmidt, C. J.; Suiciak, J. A.; Liras, S. Discovery of a novel class of phosphodiesterase 10A inhibitors and identification of clinical candidate 2-[4-(1-methyl-4-pyridin-4-yl-1*H*-pyrazol-3-yl)-phenoxymethyl]-quinoline (PF-2545920) for the treatment of schizophrenia. *J. Med. Chem.* **2009**, *52*, 5188−5196.
(21) Dedeurwaerdere, S.; Wintmolders, C.; Vanhoof, G.; Langlois, X. Patterns of brain glucose metabolism induced by phosphodiesterase 10A inhibitors in the mouse: a potential translational biomarker. *J. Pharmacol. Exp. Ther.* **2011**, *339*, 210−217.
(22) Steulet, A. F.; Bernasconi, R.; Leonhardt, T.; Martin, P.; Grunenwald, C.; Bischoff, S.; Heinrich, M.; Bandelier, V.; Maitre, L. Effects of selective dopamine D1 and D2 receptor agonists on the rate of GABA synthesis in mouse brain. *Eur. J. Pharmacol.* **1990**, *191*, 19−27.
(23) Pfeiffer, F. R.; Wilson, J. W.; Weinstock, J.; Kuo, G. Y.; Chambers, P. A.; Holden, K. G.; Hahn, R. A.; Wardell, J. R.; Alfonso, J. T. Dopaminergic activity of substituted 6-chloro-1-phenyl-2,3,4,5-tetrahydro-1*H*-3-benzazepines. *J. Med. Chem.* **1982**, *25*, 352−358.
(24) Merck, G. Preliminary notice of a new organic base in opium. *Justus Liebigs Ann. Chem.* **1848**, *66*, 125−128.
(25) Chappie, T. A.; Humphrey, J. M.; Allen, M. P.; Estep, K. G.; Fox, C. B.; Lebel, L. A.; Liras, S.; Marr, E. S.; Menniti, F. S.; Pandit, J.; Schmidt, C. J.; Tu, M.; Williams, R. D.; Yang, F. V. Discovery of a series of 6,7-dimethoxy-4-pyrrolidylquinazoline PDE10A inhibitors. *J. Med. Chem.* **2007**, *50*, 182−185.
(26) Kleiman, R. J.; Kimmel, L. H.; Bove, S. E.; Lanz, T. A.; Harms, J. F.; Romegialli, A.; Miller, K. S.; Willis, A.; des Etages, S.; Kuhn, M.; Schmidt, C. J. Chronic suppression of phosphodiesterase 10A alters striatal expression of genes responsible for neurotransmitter synthesis, neurotransmission, and signaling pathways implicated in Huntington's disease. *J. Pharmacol. Exp. Ther.* **2011**, *336*, 64−76.
(27) Giampà, C.; Laurenti, D.; Anzilotti, S.; Bernardi, G.; Menniti, F. S.; Fusco, F. R. Inhibition of the striatal specific phosphodiesterase PDE10A ameliorates striatal and cortical pathology in R6/2 mouse model of Huntington's disease. *PLoS ONE* **2010**, *5*, e13417.
(28) Tian, X.; Vroom, C.; Ghofrani, H. A.; Weissmann, N.; Bieniek, E.; Grimminger, F.; Seeger, W.; Schermuly, R. T.; Pullamsetti, S. S. Phosphodiesterase 10A upregulation contributes to pulmonary vascular remodeling. *PLoS ONE* **2011**, *6*, e18136.
(29) Sweet, L. PDE10a Inhibitors for Treating Diabetes and Related Disorders. WO2005012485A2, 2005; 28 pp.
(30) Schuit, F. Phosphodiesterase 10A Inhibitors To Amplify the Action of GLP-1-Mimetics or DPP-IV Inhibitors in Diabetes. WO2005120474A2, 2005; 25 pp.
(31) Black, S. C.; Gibbs, E. M. Phosphodiesterase 10 Inhibition as Treatment for Obesity-Related and Metabolic Syndrome-Related Conditions. WO2005120514A1, 2005; 47 pp.
(32) Pandit, J. Crystal Structure of Catalytic Domain of Rat 3′,5′-Cyclic Nucleotide Phosphodiesterase (PDE10A) Inhibitor Complex and Uses in the Discovery of Psychotherapeutic Drugs. US2005202550A1, 2005; 72 pp.
(33) Helal, C. J.; Kang, Z.; Hou, X.; Pandit, J.; Chappie, T. A.; Humphrey, J. M.; Marr, E. S.; Fennell, K. F.; Chenard, L. K.; Fox, C.; Schmidt, C. J.; Williams, R. D.; Chapin, D. S.; Siuciak, J.; Lebel, L.; Menniti, F.; Cianfrogna, J.; Fonseca, K. R.; Nelson, F. R.; O'Connor, R.; MacDougall, M.; McDowell, L.; Liras, S. Use of structure-based design to discover a potent, selective, in vivo active phosphodiesterase 10A inhibitor lead series for the treatment of schizophrenia. *J. Med. Chem.* **2011**, *54*, 4536−4547.
(34) Day, J. P.; Lindsay, B.; Riddell, T.; Jiang, Z.; Allcock, R. W.; Abraham, A.; Sookup, S.; Christian, F.; Bogum, J.; Martin, E. K.; Rae, R. L.; Anthony, D.; Rosair, G. M.; Houslay, D. M.; Huston, E.; Baillie, G. S.; Klussmann, E.; Houslay, M. D.; Adams, D. R. Elucidation of a structural basis for the inhibitor-driven, p62 (SQSTM1)-dependent intracellular redistribution of cAMP phosphodiesterase-4A4 (PDE4A4). *J. Med. Chem.* **2011**, *54*, 3331−3347.
(35) Wang, H.; Liu, Y.; Hou, J.; Zheng, M.; Robinson, H.; Ke, H. Structural insight into substrate specificity of phosphodiesterase 10. *Proc. Natl. Acad. Sci. U.S.A.* **2007**, *104*, 5782−5787.
(36) Bissantz, C.; Kuhn, B.; Stahl, M. A medicinal chemist's guide to molecular interactions. *J. Med. Chem.* **2010**, *53*, 5061−5084.
(37) Lebel, L. A.; Menniti, F. S.; Schmidt, C. J. Therapeutic use of selective PDE10A inhibitors. US2003/0032579 A1, 2003; 20 pp.
(38) Siuciak, J. A.; Chapin, D. S.; Harms, J. F.; Lebel, L. A.; McCarthy, S. A.; Chambers, L.; Shrikhande, A.; Wong, S.; Menniti, F. S.; Schmidt, C. J. Inhibition of the striatum-enriched phosphodiesterase PDE10A: a novel approach to the treatment of psychosis. *Neuropharmacology* **2006**, *51*, 386−396.
(39) Kehler, J.; Kilburn, J. P. Patented PDE10A inhibitors: novel compounds since 2007. *Expert Opin. Ther. Pat.* **2009**, *19*, 1715−1725.
(40) Allen, J. R.; Biswas, K.; Chavez, F., Jr.; Chen, N.; Demorin, F. F.; Falsey, J. R.; Frohn, M.; Harrington, P.; Horne, D.; Hu, E.; Kaller, M. R.; Kunz, R.; Monenschein, H.; Nguyen, T.; Pickrell, A.; Reichelt, A.; Rumfelt, S.; Rzasa, R.; Sham, K.; Yao, G. Pyridine and Pyrimidine Derivatives as Phosphodiesterase 10 Inhibitors. WO2010057126A1, 2010; 396 pp.
(41) Allen, J. R.; Bourbeau, M. P.; Chen, N.; Hu, E.; Kunz, R.; Rumfelt, S. Pyrazine Compounds as Phosphodiesterase 10 Inhibitors and Their Preparation and Use in the Treatment of Diseases. WO2010057121A1, 2010; 321 pp.
(42) Allen, J. R.; Chen, N.; Falsey, J. R.; Frohn, M.; Harrington, P.; Hu, E.; Kaller, M. R.; Kunz, R.; Mercede, S. J.; Nguyen, T. T.; Pickrell, A. J.; Reichelt, A.; Rumfelt, S.; Rzasa, R. M.; Sham, K.; Siegmund, A. C.; Tegley, C. M.; Yao, G. Aminopyridine, Carboxypyridine, Pyrimidine and Pyrazine Compounds as Phosphodiesterase 10 Inhibitors and Their Preparation and Use in the Treatment of PDE10-Mediated Diseases. US20100160280A1, 2010; 268 pp.
(43) Allen, J.; Frohn, M.; Harrington, P.; Pickrell, A.; Rzasa, R.; Sham, K.; Hu, E. Heteroaryloxycarbocyclyl Compounds as PDE10 Inhibitors and Their Preparation and Use in the Treatment of Diseases. WO2011143366A1, 2011; 178 pp.
(44) Allen, J.; Horne, D. B.; Hu, E.; Kaller, M. R.; Monenschein, H.; Nguyen, T. T.; Reichelt, A.; Rzasa, R. M. Preparation of Heteroaryloxyheterocyclyl and Heteroarylaminoheterocyclyl Compounds as

Phosphodiesterase 10 (PDE10) Inhibitors. WO2011143495A1, 2011; 394 pp.
(45) Allen, J. R.; Andrews, K. L.; Frohn, M. J.; Harrington, P. E.; Pickrell, A. J.; Rzasa, R. M. Preparation of Nitrogen-Containing Heterocyclic Compounds as Phosphodiesterase 10 Inhibitors. WO2011143129A1, 2011; 117 pp.
(46) Allen, J. R.; Chen, J. J.; Frohn, M. J.; Hu, E.; Liu, Q.; Pickrell, A. J.; Rumfelt, S.; Rzasa, R. M.; Zhong, W. Preparation of Nitrogen Heterocyclic Compounds Useful as 3′,5′-Cyclic Nucleotide-Specific Phosphodiesterase 10 (PDE10) Inhibitors. WO2011143365A1, 2011; 525 pp.
(47) Stange, H.; Langen, B.; Egerland, U.; Hoefgen, N.; Priebs, M.; Malamas, M. S.; Erdei, J. J.; Ni, Y. Preparation of Imidazo[5,1-*c*][1,2,4]benzotriazine Derivatives as Inhibitors of Phosphodiesterases. WO2010054260A1, 2010; 183 pp.
(48) Schmidt, C. J. Phosphodiesterase inhibitors as potential cognition enhancing agents. *Curr. Top. Med. Chem.* **2010**, *10*, 222−230.
(49) Ripka, A.; Shapiro, G.; Chesworth, R. 1,2-Disubstituted Heterocyclic Compounds as Phosphodiesterase 10 Inhibitors and Their Preparation, Pharmaceutical Compositions and Use in the Treatment of CNS Disorders and Disorders Affected by CNS Function. WO2009158393A1, 2009; 228 pp.
(50) Chesworth, R.; Shapiro, G.; Ripka, A. Di-Substituted Phenyl Compounds as Phosphodiesterase 10 Inhibitors and Their Preparation Useful in the Treatment of CNS Disorders and Disorders Affected by CNS Function. WO2009158467A2, 2009; 210 pp.
(51) Ripka, A.; Shapiro, G.; Chesworth, R. 5- and 6-Membered Heterocyclic Compounds as Phosphodiesterase Inhibitors and Their Preparation, Pharmaceutical Compositions and Use in the Treatment of CNS Disorders and Disorders Affected by CNS Function. WO2009158473A1, 2009; 172 pp.
(52) Ripka, A.; Shapiro, G.; Chesworth, R. Preparation of Vicinal Substituted Cyclopropyl Compounds as PDE-10 Inhibitors. WO2010006130A2, 2010; 70 pp.
(53) Gharat, L. A.; Narayana, L.; Yadav, P. S.; Khairatkar-Joshi, N.; Bajpai, M. Preparation of Heteroaryl Compounds as PDE10A Inhibitors. WO2011132048A1, 2011; 92 pp.
(54) Gharat, L. A.; Gajera, J. M.; Khairatkar-Joshi, N.; Bajpai, M. Tricycle Compounds as Phosphodiesterase-10 Inhibitors and Their Preparation. WO2011132051A2, 2011; 177 pp.
(55) Card, G. L.; England, B. P.; Suzuki, Y.; Fong, D.; Powell, B.; Lee, B.; Luu, C.; Tabrizizad, M.; Gillette, S.; Ibrahim, P. N.; Artis, D. R.; Bollag, G.; Milburn, M. V.; Kim, S.-H.; Schlessinger, J.; Zhang, K. Y. J. Structural Basis for the Activity of Drugs That Inhibit Phosphodiesterases. *Structure (Cambridge, MA, U. S.)* **2004**, *12*, 2233−2247.
(56) Huai, Q.; Wang, H.; Sun, Y.; Kim, H.-Y.; Liu, Y.; Ke, H. Three-Dimensional Structures of PDE4D in Complex with Roliprams and Implication on Inhibitor Selectivity. *Structure (Cambridge, MA, U. S.)* **2003**, *11*, 865−873.
(57) Xu, R. X.; Rocque, W. J.; Lambert, M. H.; Vanderwall, D. E.; Luther, M. A.; Nolte, R. T. Crystal structures of the catalytic domain of phosphodiesterase 4B complexed with AMP, 8-Br-AMP, and rolipram. *J. Mol. Biol.* **2004**, *337*, 355−365.
(58) Lingam, P. R. V. S.; Thomas, A.; Khairatkar-Joshi, N.; Bajpai, M.; Gullapalli, S.; Dahale, D. H.; Mindhe, A. S.; Rathi, V. E. Preparation of Aryl Substituted Olefinic Compounds as Phosphodiesterase 10A (PDE10A) Inhibitors. WO2011138657A1, 2011; 204 pp.
(59) Alberati, D.; Gobbi, L.; Koerner, M.; Kuhn, B.; Peters, J.-U.; Rodriguez, S. R. M.; Rogers-Evans, M.; Rudolph, M. Preparation of Pyridazinone Derivatives as PDE10A Inhibitors. WO2010063610A1, 2010; 245 pp.
(60) Alberati, D.; Koerner, M.; Kuhn, B.; Peters, J.-U.; Rodriguez, S. R. M.; Rogers-Evans, M.; Rudolph, M. Preparation of Heteroaryl Substituted Pyridazinone Derivatives as PDE10A Inhibitors. WO2010094762A1, 2010; 95 pp.
(61) Alberati, D.; Alvarez, S. R.; Bleicher, K.; Flohr, A.; Groebke, Z. K.; Koerner, M.; Kuhn, B.; Peters, J.-U.; Rudolph, M. Novel Imidazopyridines as PDE10A Inhibitors and Their Preparation and Use in the Treatment of Central Nervous System Diseases. US20110071128A1, 2011; 39 pp.
(62) Bleicher, K.; Flohr, A.; Groebke, Z. K.; Koerner, M.; Kuhn, B.; Peters, J.-U.; Rodriguez, S. R. M.; Vieira, E. Preparation of Azaheteroaryl Derivatives for Use as PDE10A Inhibitors. WO2011089132A1, 2011; 118 pp.
(63) Bleicher, K.; Flohr, A.; Groebke, Z. K.; Gruber, F.; Koerner, M.; Kuhn, B.; Peters, J.-U.; Rodriguez, S. R. M. Nitrogen Containing Heteroaryl Compounds as PDE10A Inhibitors and Their Preparation and Use in the Treatment of Diseases. WO2011154327A1, 2011; 372 pp.
(64) Pastor-Fernandez, J.; Bartolome-Nebreda, J. M.; MacDonald, G. J.; Conde-Ceide, S.; Delgado-Gonzalez, O.; Vanhoof, G. C. P.; Van, G. M. L. M.; Martin-Martin, M. L.; Alonso-De, D. S.-A. Imidazo[1,2-*b*]pyridazine Derivatives as PDE10 Inhibitors and Their Preparation, Pharmaceutical Compositions and Use in the Treatment of CNS Diseases. WO2011051342A1, 2011; 166 pp.
(65) Bartolome-Nebreda, J. M.; Conde-Ceide, S.; MacDonald, G. J.; Pastor-Fernandez, J.; Van, G. M. L. M.; Martin-Martin, M. L.; Vanhoof, G. C. P. Preparation of Imidazo[1,2-*a*]pyrazine Derivatives and Their Use for the Prevention or Treatment of Neurological, Psychiatric and Metabolic Disorders and Diseases. WO2011110545A1, 2011; 169 pp.
(66) Asproni, B.; Murineddu, G.; Pau, A.; Pinna, G. A.; Langgård, M.; Christoffersen, C. T.; Nielsen, J.; Kehler, J. Synthesis and SAR study of new phenylimidazole-pyrazolo[1,5-*c*]quinazolines as potent phosphodiesterase 10A inhibitors. *Bioorg. Med. Chem.* **2011**, *19*, 642−649.
(67) Kehler, J.; Ritzen, A.; Langgård, M.; Petersen, S. L.; Farah, M. M.; Bundgaard, C.; Christoffersen, C. T.; Nielsen, J.; Kilburn, J. P. Triazoloquinazolines as a novel class of phosphodiesterase 10A (PDE10A) inhibitors. *Bioorg. Med. Chem. Lett.* **2011**, *21*, 3738−3742.
(68) Ritzen, A.; Kehler, J.; Langgaard, M.; Nielsen, J.; Kilburn, J. P.; Farah, M. M. Novel Phenylimidazole Derivatives as PDE10A Enzyme Inhibitors for Treating Neurodegenerative Disorder, Psychiatric Disorder, or Drug Addiction. WO2009152825A1, 2009; 91 pp.
(69) Ritzen, A.; Kehler, J.; Langgaard, M.; Nielsen, J.; Kilburn, J. P.; Farah, M. M. Novel Phenylimidazole Derivatives as PDE10A Enzyme Inhibitors for Treating Neurodegenerative Disorder, Psychiatric Disorder, or Drug Addiction. US20100016303A1, 2010; 34 pp.
(70) Pueschl, A.; Nielsen, J.; Kehler, J.; Kilburn, J. P.; Marigo, M.; Langgaard, M. Preparation of Heteroaromatic Aryl Triazole Derivatives as PDE10A Enzyme Inhibitors for Treating Neurodegenerative Disorders, Psychiatric Disorders, or Drug Addiction. WO2011072697A1, 2011; 68 pp.
(71) Pueschl, A.; Nielsen, J.; Kehler, J.; Kilburn, J. P.; Marigo, M.; Langgaard, M. Preparation of 2-Arylimidazole Derivatives as PDE10A Enzyme Inhibitors for Treating Neurodegenerative Disorders, Psychiatric Disorders, and Drug Addiction. WO2011072696A1, 2011; 62 pp.
(72) Pueschl, A.; Nielsen, J.; Kehler, J.; Kilburn, J. P.; Marigo, M.; Langgaard, M. Phenylimidazole Derivatives Comprising an Ethynylene Linker as Phosphodiesterase 10A Enzyme Inhibitors. WO2011072695A1, 2011; 48 pp.
(73) Breslin, M. J.; Coleman, P. J.; Cox, C. D.; Raheem, I. T.; Schreier, J. D. Preparation of Alkoxy-tetrahydro-pyridopyrimidine PDE10 Inhibitors. WO2010138430A1, 2010; 70 pp.
(74) Hostetler, E.; Cox, C. D.; Fan, H. Radiolabeled PDE10 Inhibitors. WO2010138577A1, 2010; 71 pp.
(75) Cox, C. D.; Bunda, J. L.; Flores, B. A.; Shipe, W. Pyrimidinones as Phosphodiesterase 10 Inhibitors for the Treatment of Central Nervous System Disorders. WO2010138585A1, 2010; 68 pp.
(76) Breslin, M. J.; Coleman, P. J.; Cox, C. D.; Raheem, I. T.; Schreier, J. D. Preparation of Aminotetrahydropyridopyrimidine Derivatives for Use as PDE10 Inhibitors. WO2011022213A1, 2011; 48 pp.
(77) Breslin, M. J.; Cox, C. D.; Raheem, I. T. Aryl Aminopyridine Phosphodiesterase 10 Inhibitors for Treatment of Central Nervous System Disorders. WO2011053559A1, 2011; 47 pp.
(78) Cox, C. D.; Raheem, I. T.; Flores, B. A.; Whitman, D. B. 7-Azaquinazolines as PDE10 Inhibitors. US20110319409A1, 2011; 23 pp.

(79) Morimoto, H.; Sakamoto, T.; Himiyama, T.; Kawanishi, E.; Matsumura, T. Preparation of Substituted Pyrimidine Derivatives for Use as PDE10 Inhibitors. WO2010030027A1, 2010; 117 pp.
(80) Kawanishi, E.; Matsumura, T. Preparation of Trisubstituted Pyrimidines as Phosphodiesterase PDE10 Inhibitors. WO2010027097A1, 2010; 85 pp.
(81) Kawanishi, E.; Hongu, M.; Tanaka, Y. Preparation of Pyrazolopyrimidine Compounds and Their Use as Therapeutic PDE10 Inhibitors. WO2011105628A1, 2011; 139 pp.
(82) Gage, J. L.; Onrust, R.; Johnston, D.; Osnowski, A.; MacDonald, W.; Mitchell, L.; Ürögdi, L.; Rohde, A.; Harbol, K.; Gragerov, S.; Dormán, G.; Wheeler, T.; Florio, V.; Cutshall, N. S. *N*-Acylhydrazones as inhibitors of PDE10A. *Bioorg. Med. Chem. Lett.* **2011**, *21*, 4155−4159.
(83) Cutshall, N. S.; Gage, J. L.; Wheeler, T. N.; Little, T. L. Preparation of Phenylfuranylheteroarylphenylethanone Derivatives and Analogs for Use as PDE10 Inhibitors. WO2011112828A1, 2011; 140 pp.
(84) Ho, G. D.; Yang, S.-W.; Smith, E. M.; McElroy, W. T.; Basu, K.; Smotryski, J.; Tan, Z.; McKittrick, B. A.; Tulshian, D. B. Preparation of Substituted Pyrazoloquinolines and Derivatives Thereof. WO2010062559A1, 2010; 129 pp.
(85) Yang, S.-W.; Smotryski, J.; McElroy, W. T.; Tan, Z.; Ho, G.; Tulshian, D.; Greenlee, W. J.; Guzzi, M.; Zhang, X.; Mullins, D.; Xiao, L.; Hruza, A.; Chan, T.-M.; Rindgen, D.; Bleickardt, C.; Hodgson, R. Discovery of orally active pyrazoloquinolines as potent PDE10 inhibitors for the management of schizophrenia. *Bioorg. Med. Chem. Lett.* **2012**, *22*, 235−239.
(86) Ho, G. D.; Smith, E. M.; Kiselgof, E. Y.; Basu, K.; Tan, Z.; McKittrick, B.; Tulshian, D. Preparation of Substituted Triazolopyridines and Analogs as Phosphodiesterase 10 (PDE10) Inhibitors. WO2010117926A1, 2010; 59 pp.
(87) Ho, G. D.; Seganish, W. M.; Tulshian, D. B.; Timmers, C. M.; Rijn, R. D. V.; Loozen, H. J. J. 5,6-Dihydroimidazo[5,1-*a*]isoquinoline Derivatives as PDE10 Inhibitors and Their Preparation and Use for the Treatment of PDE10-Modulated Diseases. WO2011008597A1, 2011; 50 pp.
(88) Campbell, J. E.; Hewitt, M. C.; Jones, P.; Xie, L. Preparation of Heteroaryl Compounds Useful in the Treatment of CNS, Metabolic and Other Diseases. WO2011150156A2, 2011; 233 pp.
(89) Taniguchi, T.; Kawada, A.; Kondo, M.; Quinn, J. F.; Kunitomo, J.; Yoshikawa, M.; Fushimi, M. Preparation of Pyridazinone Compounds as Phosphodiesterase 10A Inhibitors for Preventing and Treating Schizophrenia. US20100197651A1, 2010; 175 pp.
(90) Taniguchi, T.; Yoshikawa, M.; Miura, K.; Hasui, T.; Honda, E.; Imamura, K.; Kamata, M.; Kamisaki, H.; Quinn, J. F.; Raker, J.; Camara, F.; Wang, Y. Preparation of Fused Heterocyclic Compounds as Phosphodiesterase 10A Inhibitors for Preventing and Treating Schizophrenia. WO2011163355A1, 2011; 386 pp.
(91) Grimwood, S.; Hartig, P. R. Target site occupancy: emerging generalizations from clinical and preclinical studies. *Pharmacol. Ther.* **2009**, *122*, 281−301.
(92) Celen, S.; Koole, M.; De Angelis, M.; Sannen, I.; Chitneni, S. K.; Alcazar, J.; Dedeurwaerdere, S.; Moechars, D.; Schmidt, M.; Verbruggen, A.; Langlois, X.; Van Laere, K.; Andrés, J. I.; Bormans, G. Preclinical evaluation of 18F-JNJ41510417 as a radioligand for PET imaging of phosphodiesterase-10A in the brain. *J. Nucl. Med.* **2010**, *51*, 1584−1591.
(93) Andrés, J.-I.; De Angelis, M.; Alcázar, J.; Iturrino, L.; Langlois, X.; Dedeurwaerdere, S.; Lenaerts, I.; Vanhoof, G.; Celen, S.; Bormans, G. Synthesis, in vivo occupancy, and radiolabeling of potent phosphodiesterase subtype-10 inhibitors as candidates for positron emission tomography imaging. *J. Med. Chem.* **2011**, *54*, 5820−5835.
(94) Andres-Gil, J. I.; De, A. M.; Bormans, G. M. R.; Celen, S. J. L. Radiolabelled PDE10 Ligands. WO2011051324A1, 2011; 72 pp.
(95) Tu, Z.; Fan, J.; Li, S.; Jones, L. A.; Cui, J.; Padakanti, P. K.; Xu, J.; Zeng, D.; Shoghi, K. I.; Perlmutter, J. S.; Mach, R. H. Radiosynthesis and in vivo evaluation of [^{11}C]MP-10 as a PET probe for imaging PDE10A in rodent and non-human primate brain. *Bioorg. Med. Chem.* **2011**, *19*, 1666−1673.
(96) Chen, Y.; Spangler, W.; Kreulen, J.; et al. Presented at IEEE International Conference on Data Mining (ICDM), 2009.
(97) Wager, T. T.; Hou, X.; Verhoest, P. R.; Villalobos, A. Moving beyond rules: the development of a central nervous system multiparameter optimization (CNS MPO) approach to enable alignment of druglike properties. *ACS Chem. Neurosci.* **2010**, *1*, 435−449.
(98) Bemis, G. W.; Murcko, M. A. The properties of known drugs. 1. Molecular frameworks. *J. Med. Chem.* **1996**, *39*, 2887−2893.
(99) Medina-Franco, J. L.; Martinez-Mayorga, K.; Giulianotti, M. A.; Houghten, R. A.; Pinilla, C. Principal component analysis. *Curr. Comput.-Aided Drug Des* **2008**, *4*, 322−333.
(100) Accelrys, Inc., San Diego, CA, U.S.
(101) TIBCO Software, Inc. Somerville, MA, U.S.